NATIONAL ADVISORY COMMITTEE FOR AERONAUTICS

TECHNICAL NOTE 3298

A LOW-DENSITY WIND-TUNNEL STUDY OF SHOCK-WAVE STRUCTURE AND RELAXATION PHENOMENA IN GASES

By F. S. Sherman

University of California

Washington
July 1955

H

NATIONAL ADVISORY COMMITTEE FOR AERONAUTI

TECHNICAL NOTE 3298

A LOW-DENSITY WIND-TUNNEL STUDY OF SHOCK-WAVE STRUCTURE AND RELAXATION PHENOMENA IN GASES

By F. S. Sherman

SUMMARY

The profiles and thicknesses of normal shock waves of moderate strength have been determined experimentally in terms of the variation of the equilibrium temperature of an insulated transverse cylinder in free-molecule flow. The shock waves were produced in a steady state in the jet of a low-density wind tunnel, at initial Mach numbers of 1.72 and 1.82 in helium and 1.78, 1.85, 1.90, 1.98, 3.70, and 3.91 in air. The shock thickness, determined from the maximum slope of the cylinder temperature profile, varied from 5 to $3\frac{1}{2}$ times the length of the Maxwell mean free path in the supersonic stream. A comparison between the experimental shock profiles and various theoretical predictions leads to the tentative conclusions that: (1) The Navier-Stokes equations are adequate for the description of the shock transition for initial Mach numbers up to 2, and (2) the effects of rotational relaxation times in air can be accounted for by the introduction of a "second" or "bulk" viscosity coefficient equal to about two-thirds of the ordinary shear viscosity.

INTRODUCTION

A precise experimental determination of the structure and thickness of the normal shock wave is of fundamental interest in the study of gas dynamics because it does much to define the usefulness of the Navier-Stokes equations, or of any alternative set of equations, for predicting the behavior of a very nonuniform gas. In addition, the observed nature of the shock wave sheds considerable light on the magnitude and character of so-called "relaxation effects" associated with the finite time required to obtain equipartition of energy among the translational and internal motions of a polyatomic molecule.

The advantages of the normal shock wave as an object of both experimental and theoretical study are:

(1) The one-dimensionality of the flow

(2) The lack of dependence of the internal shock-wave structure upon the nature of boundary conditions at a fluid-solid interface

(3) The relatively high degree of nonuniformity of the flow, which is sufficient in a shock of moderate strength to cause measurable differences in the profiles predicted by various theories

(4) The dependence of the degree of nonuniformity, to be defined by dimensionless values of the stress and heat flux in the fluid, or by the fractional variation of mean flow properties over the length of a molecular mean free path, upon a single shock-strength parameter

It is the last-named property of the shock wave which suggests the use of the low-density wind tunnel for experimental investigation. Since the pertinent scale of distance in the shock wave is the mean-free-path length, use of the low-density gas stream with its relatively long mean free paths will relieve the most troublesome difficulty of shock-wave-structure experiments - the accurate resolution of the very small shock thicknesses found in normal-density wind tunnels and shock tubes. Whereas the thickness of a shock in air at a Mach number of 2 may be 1.1×10^{-5} inch at standard temperature and pressure (conditions upstream of the wave), the same shock (i.e., same Mach number) will have a thickness of 0.047 inch in the no. 3 low-density wind tunnel.

The theoretical problems involved in calculating the profile of the steady normal shock wave have been treated in a literature[1] which originated with papers by Rankine, Rayleigh, and Taylor. Subsequently, the treatment of the problem by use of the Navier-Stokes equations and the assumption of a perfect gas has been brought to a satisfactory completion, so that one may now predict the effects of variation of all the significant parameters (Mach number, Prandtl number, and specific-heats ratio) and take into account the temperature dependence of the viscosity, thermal conductivity, and Prandtl number. Even weak relaxation effects have been accounted for in a recent paper (ref. 16) through the introduction of a second viscosity coefficient (also called bulk, volume, or compression viscosity) which is assumed to have the same temperature dependence as the ordinary shear viscosity.

Several authors among those listed have concluded on the basis of their calculations that the flow within any but the weakest shocks is so nonuniform that it cannot be accurately described by the Navier-Stokes equations. The equations which are usually suggested as improvements are those derived from a kinetic-theory viewpoint, by the methods of Enskog, Chapman, Burnett, and Grad (see, e.g., refs. 17 and 18). These

---

[1]See references 1 to 16 for a representative but not exhaustive bibliography.

more complicated equations have been derived for a monatomic gas only and have been applied to the calculation of shock-wave profiles in three recent papers (refs. 7, 12, and 15) with results which were concluded, particularly by Grad and Zoller, to be preferable to the Navier-Stokes results for Mach numbers greater than about 1.3. The basis for the preference is largely that the predicted shock thicknesses are relatively greater according to the more complicated theories. Partly because of the plausible nature of the derivation of the higher order kinetic-theory equations, and partly because some of the comparisons of shock thicknesses calculated from them and from the Navier-Stokes equations were improperly drawn, the Navier-Stokes equations have fallen lately into some disrepute. On the other hand, it may be emphasized that this line of thinking has been to date almost entirely inspired by theory, since little or no experimental information is available on flows which are sufficiently nonuniform to make a measurable difference in the predictions of various theories. Even the purely theoretical trend of thought has encountered some rebuttal, notably by Gilbarg and Paolucci (ref. 16).

Although the usual experimental study of relaxation phenomena in polyatomic gases has to do with the absorption and anomalous velocity dispersion of forced ultrasonic waves in a gas,[2] the effects of lagging internal energies are equally evident in the structure of a normal shock wave. If the relaxation times are so small that their effects can be represented fluid mechanically by a nonzero value of the bulk viscosity (refs. 7 and 16), analysis shows that the shock thickness is increased by the relaxation effect, quite measurably for even the smallest values for bulk viscosity given in the ultrasonic literature, although the shape of the shock profile is not greatly altered. If, on the other hand, the lag of internal energies is so severe that it is appropriate to describe the gas within the shock as a reacting mixture with sensibly different temperatures for the translational and internal motions, then it may be expected that the shock profile will assume a shape considerably different from that of a shock in a monatomic gas. The profile for the relaxing gas would be characterized by a zone of comparatively rapid transition for the translational motions mixed with and followed by a longer zone of adjustment of energy between the translational and internal degrees of freedom (refs. 20 to 22).

The experimental investigation reported herein is not the first to be directed toward a determination of the structure and thickness of shock waves or to consider the shock wave as a useful source of information concerning relaxation effects. Greene, Cowan, and Hornig of Brown University have for several years been developing a remarkable program of similar intent, utilizing a measurement of the optical reflectivity of shock fronts

---

[2]Reference 19 gives a good summary of this work.

passing through a shock tube at atmospheric pressure and above (refs. 23 to 25). The present studies were undertaken because the experimental method and tools are entirely distinct from those employed by Greene, Cowan, and Hornig and seem to offer certain advantages in directness and detail of measurement and in accuracy and interpretation of results.

This work was conducted at the University of California under the sponsorship and with the financial assistance of the National Advisory Committee for Aeronautics.

SYMBOLS

c_p	specific heat at constant pressure
c_v	specific heat at constant volume
j	number of excited internal degrees of freedom of a molecule
L_*	reference length, ft
M_1	Mach number upstream of shock wave
Pr	Prandtl number
p	pressure, lb/sq ft
T_o	wind-tunnel reservoir temperature, ^oR
T_*	reference temperature, ^oR, $\left(\frac{j+3}{j+4}\right)T_o$
T_w	wire temperature, ^oR
t_w	dimensionless, normalized wire temperature
u	macroscopic flow velocity, fps
w	dimensionless, normalized flow velocity
x	distance along flow, ft
y	dimensionless distance along flow

γ specific-heats ratio, c_p/c_v

δ "area" shock thickness (fig. 10), ft, or units of y

δ_m "maximum-slope" shock thickness (fig. 10), ft, or units of y

δ_{ij} Kronecker delta function

ϵ dimensionless shock-strength parameter

κ bulk viscosity modulus, lb-sec/sq ft; defined by Navier-Stokes formulation for viscous stress

$$p_{ij} = -p\delta_{ij} + \mu\left(\frac{\partial u_i}{\partial x_j} + \frac{\partial u_j}{\partial x_i} - \frac{2}{3}\delta_{ij}\frac{\partial u_\alpha}{\partial x_\alpha}\right) + \kappa\delta_{ij}\frac{\partial u_\alpha}{\partial x_\alpha}$$

Λ_1 Maxwell mean free path upstream of shock, ft

μ shear viscosity modulus, lb-sec/sq ft

ξ_x x-component of total molecular velocity, fps

ρ density, slugs/cu ft

Other symbols, used in the appendixes, are defined where they appear.

EXPERIMENTAL METHOD

The essence of the experimental method can be described very briefly. A normal shock wave is produced in a steady state by introducing an appropriately designed obstacle into the supersonic jet of the low-density wind tunnel. The shock-wave profile is then recorded in terms of the variation in the equilibrium temperature of a small-diameter wire oriented parallel to the plane of the shock, as the wire is traversed through the shock zone. As a consequence of the relatively long mean free paths characterizing the low-density wind-tunnel flows, temperature-sensitive wires may be obtained with diameters sufficiently small compared with the mean-free-path length so that the presence of the wire in the shock zone does not disturb the macroscopic flow pattern. Under such conditions of free-molecule flow, it is possible to make a theoretical calculation of the wire temperature at any point in the gas at which the molecular distribution function is known and so to relate the wire temperature profile of a shock to the velocity or density profile, and so forth. This availability of a free-molecule-flow hot-wire anemometer for low-density wind

tunnels was first noted by Tsien (ref. 26). The method is complicated experimentally by problems of producing a shock which approximates closely the theoretical model, in which the limiting flows upstream and downstream of the shock are perfectly uniform, and by problems of minimizing extraneous thermal exchanges to the wire due to radiation and metallic conduction. These are discussed in later sections and in appendix A.

Theoretical interpretations of the results stem largely from the basic work by Stalder and associates (refs. 27 to 29), who investigated the free-molecule cylinder in a uniform stream, and from recent work by Bell (ref. 30), who considered the effects of nonuniformities in the flow. Appendixes B and C are devoted to application of their methods to the prediction of wire temperature profiles for comparison with the experimental results.

EXPERIMENTAL APPARATUS AND PROCEDURE

Development of Apparatus

Shock holders.- The type of shock-producing device which was finally developed is shown in figure 1. It consists of a thin-walled circular cylinder or cone frustum which is immersed in the uniform portion of the wind-tunnel jet. The cylinder is alined carefully with its axis parallel to the direction of flow and is provided with some movable device with which to vary the open area of its downstream end. When the downstream opening is completely plugged, a shock stands detached as in front of an impact tube or other blunt body. As shown in figure 2, gradual withdrawal of the plugging device decreases the detachment distance and the curvature of the central portion of the shock wave until a plane shock wave is obtained at the entry of the cylinder. (Actually, the shock is swallowed in the last picture shown in fig. 2.) The ideal shock holder of this type should behave in the following manner: The shock should be held stably and exactly across the mouth of the cylinder, so that it will be plane and normal to the flow. The shock should be followed by a region of uniform subsonic flow of sufficient extent to permit identification of any suspected relaxation effects downstream of the shock and then by some sort of throat section which will isolate this region from the low-pressure region of reexpanded flow behind the shock holder.

In the development of the shock holder, use was made of the air-afterglow flow-visualization technique (ref. 31), of a static-pressure tap on the inside of the shock holder near the rear, and of a number of very small impact-pressure tubes. The latter instruments are sensitive to the transition of flow properties through the shock because of varying viscous and rarefaction effects which are too complicated to be subject to theoretical prediction. Since the impact tubes were not small

enough to enjoy free-molecule flow, they disturbed the shock wave as they passed through, as may be seen in figure 3. The nature of impact-pressure traces recorded with a 0.043-inch-diameter tube is shown in figure 4, along with a family of curves showing the influence of the probe position upon the pressure recorded at the shock-holder wall tap.

As is evident from figures 2 and 5, different types of choking devices were incorporated with the shock holder. The grid shown in figure 5 seemed most satisfactory and was used in the final experiments.

One final item to be noted in the shock-holder design is the slotting of the leading edge to permit passage of the measuring wire. It appeared possible to make these slots wide enough to permit good clearance for the wires, without disturbing the nature of the shock held across the entry plane.

Limited use was made of another type of shock producer, namely, a large transverse cylinder, which produces a detached shock that is locally normal in the vicinity of the stagnation streamline but is followed by a decelerating flow.

Free-molecule equilibrium-temperature probe.- Both temperature-sensitive resistance wires and butt-welded thermocouples were used to fulfill the function of the free-molecule equilibrium-temperature probe (fig. 6). The resistance wires have the advantage of availability in very small diameters and in very strong metals, so that they may enjoy free-molecule flow over a wide range of wind-tunnel flow conditions and so that they may be held straight in tension for purposes of alinement and location. Since the resistance-wire response is to an integrated average temperature over the measuring length, a serious problem of the minimization of thermal end losses must be met. This was done in the present experiments by introducing separate potential leads to isolate and measure the resistance of a relatively short central section of the current-bearing wire. The potential leads were of the same diameter and material (0.00025-inch tungsten) as the current wire and were very neatly joined to the latter in a made-to-order unit furnished by Flow Corporation of Cambridge, Massachusetts. The measuring length was about 1/2 inch, or approximately the central third of the diameter of the shock-holder entry. The potential leads and current wire were oriented in a plane parallel to the plane of the shock, and there was no indication that this distortion of the probe geometry from that of a simple transverse cylinder had any effect on the equilibrium temperature.

Thermocouple probes have the advantage of being temperature sensitive only at the junction but are not easily available in diameters less than 0.002 inch because of the mechanical inferiority of most thermocouple metals and the difficulty of producing the butt-welded or neatly lap welded junction. The range of wind-tunnel operation which will produce

free-molecule flow about a wire of this diameter is quite restricted. Early models of the thermocouple probe were similar to that shown in figure 5. A measuring section 3/4 inch long, with a junction in the center, was held transverse to the flow by its own ends, which extended downstream for 1/2 inch before passing into small supporting tubes of drawn Pyrex. This arrangement was inferior from a point of view of wire straightness and of thermal end losses and was abandoned when the feasibility of slotting the shock holder was discovered. The final thermocouple probe was a simple wire of 0.002-inch iron and constantan, neatly lap welded at the center of a 6- or 7-inch length (fig. 6(b)).

Wire traverse.- The final arrangement for support and locomotion of the equilibrium-temperature probes is shown in figure 7. The ends of the thermocouple wires, or special heavier wires attached to the ends of the tungsten resistance thermometer, passed through ceramic insulators mounted on a light spring-steel yoke and were soldered into the measuring circuit. The yoke could be spread apart by a differential screw turnbuckle, to place the wires in tension, and it was in turn mounted on a carriage which could be run back and forth along the direction of flow by a small electric motor. The supposedly constant speed at which this traverse moved was 1 inch per 40 minutes, but tests showed that this varied slightly over the period of one revolution of the drive motor. The position of the wire at any time was given by a dial indicator attached rigidly to the upstream wall of the test chamber and bearing against the movable base of the wire support yoke.

Wind-Tunnel Facilities

The low-density wind tunnel is the no. 3 wind tunnel at Berkeley, a continuous-flow, nonreturn, open-jet type (ref. 32). The two nozzles which were employed for the present tests are designated as nozzle 6 ($1.8 < M < 2.2$) and nozzle 8 ($3.7 < M < 4.1$)(ref. 33). The gas intake to the tunnel is either directly from the room, through activated-alumina driers, or from bottled gas. In the latter case, the bottled gas can be rendered very dry by running it through a refrigerated trap (ref. 31) at about 125 pounds per square inch gage, yielding dew points lower than -100° F as measured by an Alnor Type 7000L Dew-Pointer. Extra-dry air can be obtained by running air from a compressor through this trap. With regard to the ultimate purity of the gases in the wind-tunnel jet, very little of a quantitative nature can be said, because of the unknown influence of small leaks in the wind-tunnel shell or in the line between the wind tunnel and the drier or of outgassing. In general, no special precautions were taken to insure gas purity during the present tests, since a few experiments in which nitrogen was kept as pure as possible yielded results which were indistinguishable from those obtained with room air.

Since the no. 3 wind tunnel is not equipped with special nozzles for helium, nozzle 6 was used in this capacity. The flow produced in this manner was somewhat less uniform than the air flow for which the nozzle was designed, and the nozzle calibration in helium is correspondingly less certain than that in air.

As mentioned previously, the chief feature of the no. 3 wind tunnel which is of interest to the shock-wave study is the production of long molecular mean free paths. In figure 8 the mean-free-path length in the free stream is plotted, in inches, versus the weight rate of gas flow in the two nozzles. Note that the longer mean free paths occur in the lower Mach number nozzle, which fact made it easier to obtain shock-wave traces in nozzle 6 and accounts somewhat for the scanty data obtained for the higher Mach number flows. Another factor in the wind-tunnel performance which limited the scope of tests in the higher Mach number nozzle was a slight fluctuation in the test-section pressure which became serious at flow rates greater than 10 pounds per hour, making it impossible to produce a perfectly steady shock. Something of this nature occurred also in nozzle 6 but seemed to be the fault of the shock holder, whereas even a detached shock off a transverse cylinder was unsteady at high flow rates in nozzle 8.

Technique and Schedule of Final Experiments

After a fairly extended period of preliminary and developmental experiments, a series of final tests was performed. The testing procedure was very simple once a shock holder and thermocouple or resistance-wire probe had been installed and alined. This alinement was easily achieved when a thermocouple was used, since the shock holder was mounted in a manner allowing delicate adjustment of its height and inclination and since there were only two slots in the shock holder for the wire to clear. The resistance-wire-thermometer alinement, requiring clearances in four slots, was somewhat more tedious and was accomplished by adjusting both the shock-holder orientation and the positions of the ends of the fine tungsten wires. The latter adjustment was achieved by bending the heavy wires which were attached to each tail of the tungsten wires.

When the wind tunnel was ready to be operated, the free-molecule cylinder was first placed in the entry plane of the shock holder to provide an indication of proper location of the shock wave. With flow established at a Mach number and pressure level known to be appropriate to the particular shock holder in use, the shock-holder choking grid would be set to give first a detached shock and then a swallowed one. The wire-temperature indications for these two conditions corresponded approximately to the downstream and upstream limits of the shock-wave profile, and, when the choking grid was further manipulated to make the temperature of the wire (still in the entry plane) nearly equal to the average of these end

readings, the shock was considered to be properly placed. One factor due to the influence which the shock position had on the balance between jet static and test-chamber pressures complicated this procedure. Since the shock holder captured a sizable fraction of the uniform portion of the jet, there was a considerable interaction between the shock position and the aforementioned pressure balance, making it necessary to adjust the two more or less simultaneously.

Once the shock had been positioned, the wire temperature was observed over a period of time, in order to make certain that the shock was stationary. Then the measuring wire was run downstream until a definite indication of the uniform flow downstream of the shock was reached. From this point, the shock profile was traced out in the upstream direction by two different techniques, one appropriate to the resistance thermometer and the other, to the thermocouple.

Shock traces with a resistance thermometer.- The resistance wire was fed a constant current of 0.2 milliampere, obtained from a 3-volt dry cell, a fixed 10,000-ohm resistor, and a 0- to 12,500-ohm variable resistor in series. The potential drop across the temperature-measuring section of the wire was measured with a Rubicon hand-balancing potentiometer and sensitive galvanometer (Leeds and Northrup, 0.44 microvolt per millimeter), while the wire current was monitored by a Weston Model 31 milliammeter. The potentiometer readings were converted to temperatures by use of a linear formula with a temperature coefficient of resistance which was determined by the wire manufacturer from calibrations performed on samples from the same spool of wire. According to this calibration the least count of the Rubicon corresponded to about 0.1° F when the wire current was 0.2 milliampere.

While the wire temperature was being measured in the above manner, the stagnation temperature of the flow was measured by an iron-constantan thermocouple located in the upstream reservoir chamber. Before each run, an initial reading of wire resistance versus thermocouple temperature was taken at no-flow conditions, with a sufficiently high gas pressure to make the wire temperature correspond to the true gas temperature. The scatter of these no-flow readings from day to day gave some idea of the probable error of determination of the absolute temperature of the wire due to calibration drifts, instrument errors, and so forth.

During the tracing of a shock profile, the potential drop across the resistance wire and the wire position were recorded at a sufficient number of points, the spacing of which was determined by the mean-free-path length, to give a satisfactory definition of the shock profile and thickness, as shown in figures 9(a) to 9(h). The time required for this was about an hour per shock wave.

Traces with thermocouple wire.- When thermocouple probes were used, the difference in thermal electromotive forces generated by the probe junction and by an identical junction placed in the stagnation chamber was automatically recorded by a Brown Electronik X-Y function plotter. The recorder chart was driven at constant speed by a small motor wired in parallel with the motor on the wire traverse. Distance on the chart was converted to distance traveled by the wire by assuming wire and chart speeds to be constant at values measured with a stop watch. Each shock-wave trace was recorded in both the upstream and downstream directions, and when the recorder sensitivity was adjusted to the maximum limit for stable pen motion the hysteresis between forward and rearward running traces amounted to a few thousandths of an inch of wire travel. The stagnation temperature was recorded separately with the same thermocouple as was used with the resistance wire.

Schedule of final experiments.- The final data which are reported herein were taken at initial (or upstream) Mach numbers of 1.72 and 1.82 in helium and 1.78, 1.85, 1.90, 1.98, 3.70, and 3.91 in air.

REDUCTION OF DATA

The dimensionless variables introduced for analysis of the data were suggested for the most part by Grad's analysis (ref. 15). The distance in the direction of the flow is converted to a variable y, defined by

$$y = \left(\frac{j + 4}{j + 5}\right)\frac{\left(\frac{3\kappa}{4\mu} + 1\right)\mathrm{Pr}}{2 + (j + 3)\left(\frac{4}{3} + \frac{\kappa}{\mu}\right)\mathrm{Pr}}\frac{\epsilon x}{L_*}$$

This variable is discussed in appendix B. In the formula for y, x is the measured distance, L_* is a reference length having the same units as x, and ϵ is a parameter indicating the strength of the shock; L_* and ϵ are computed from more familiar variables by the equations

$$L_* = \frac{1}{\rho u}\left(\frac{3\kappa}{4\mu} + 1\right)\mu(T_*)$$

$$T_* = \frac{j + 3}{j + 4}T_0$$

$$\epsilon = \frac{(j^2 + 8j + 15)(M_1^2 - 1)}{(j + 3) + (j + 5)M_1^2}$$

The gas properties which have been assumed for the reduction of the data are as follows: For helium:

$$j = 0, \quad Pr = 2/3, \quad \kappa = 0$$

and for air:

$$j = 2, \quad Pr = 3/4, \quad \kappa = 2\mu/3$$

The temperature dependence of μ was taken from references 34 and 35. Table I gives a listing of the calculated values of y/x for each flow setting at which a final shock profile was traced, along with other variables needed to describe the flow.

If one prefers the upstream mean free path Λ_1 as a reference length, he may convert the abscissa of the shock profiles y to x/Λ_1 by dividing y by y/x and then by Λ_1. Both of the last-named quantities are listed for each flow setting in table I.

The free-molecule cylinder temperature is determined from the calibration of the thermocouple or resistance wire and is made dimensionless by forming its ratio to the measured stagnation temperature. This ratio is then normalized to run from 1 to -1, in the manner applied to the theoretical profiles in appendix B, by use of the formula

$$t_w = 2\left[\frac{\frac{T_w}{T_o} - \left(\frac{T_w}{T_o}\right)_2}{\left(\frac{T_w}{T_o}\right)_1 - \left(\frac{T_w}{T_o}\right)_2}\right] - 1$$

in which subscripts refer to conditions at the upstream (1) and downstream (2) limits of the shock zone. This variable artificially cancels the effects of calibration differences and radiation and end losses, as well as the theoretical variation in temperature spread across the shock, simplifying comparisons of experiment with theory or of one experiment with another. Introduction of the variable is in keeping with the aim of the present investigation, since the normalization does not influence those characteristics of the shock profile (i.e., shape and thickness) which are of principal interest herein. The normalized temperature can be formed only for the traces of normal shocks produced in the hollow shock holder, because the detached shock traces have no point of zero slope to serve as a reference level on the downstream side.

The normal-shock traces are presented as graphs of t_w versus y, based upon the step-by-step data of the resistance-wire measurements and upon a curve faired smoothly through the middle of the hysteresis loop of the thermocouple traces. In drawing the latter curve, an attempt was made to remove the effects of the small periodic speed variation in the wire-traverse motor. The origin for the variable y is taken arbitrarily at about the point at which t_w equals zero.

The shock thicknesses are determined graphically from the curves of t_w versus y by both the maximum-slope method (Prandtl's definition) and the area method recently suggested by Grad. Figure 10 compares the two definitions, which yield the same numerical values only if the shock profile is a straight line. For any other profile the area thickness is greater than the maximum-slope thickness; for example, for the zero-strength profile (see appendix B) the area thickness is 2.77 in units of y, while the maximum-slope thickness is 2. In what follows, the area thickness will be designated by δ and the maximum-slope thickness, by δ_m.

EXPERIMENTAL RESULTS

Free-Molecule Probe Response in a Uniform Stream

Both theory and previous experiment (refs. 27 to 29) have shown that a cylinder which is a perfect heat conductor internally but is totally insulated from radiation and end losses, if placed with its axis perpendicular to a uniform stream of gas in which the mean-free-path length is several times the cylinder diameter, is heated by the stream to a temperature which is a function only of the local Mach number and static temperature and of the number of excited degrees of freedom of the gas molecules. For a stream with constant stagnation temperature, the cylinder temperature increases fairly rapidly with Mach number up to about $M = 2$, after which the response is quite insensitive to further increase in M. The first important results of the present experiments demonstrate the extent to which this behavior was found in the wires which were used as shock-wave probes. These wires were different from those with which the free-molecule theory was tested by Stalder, Goodwin, and Creager (ref. 29) in that no attempt was made to combat thermal end losses by artificial end temperature control. Aside from the special arrangement of the resistance-wire thermometer, with extra potential leads to isolate a central portion of the current wire, the present wires depended only on a high length-diameter ratio to reduce end-loss effects. The results obtained are seen in figure 11, in which the ratio of measured wire temperature to measured stagnation temperature is compared with the theoretical ratio for a perfectly insulated cylinder. This figure shows all experimental points for which the Knudsen number was greater than about 5 lying as close to the theoretical curves as can be expected in view of probable errors in measurement. (Exceptions to this statement, for which no explanation has been found, exist in the case of certain data for helium at supersonic Mach numbers.) As the Knudsen number drops below 5, the points tend to drop below the theoretical curve because of a lack of fully developed free-molecule flow.

As a consequence of the results shown in figure 11 it is thought that the wires used in this experiment behaved as insulated cylinders in fully developed free-molecule flow, for all wind-tunnel conditions encountered, as long as the mean free path in the vicinity of the wire was at least 5 wire diameters long.

Operation of Normal Shock Holders

Experimental difficulties which were encountered in the attempt to realize the ideal shock-holder behavior described earlier appeared to be of two kinds, both probably traceable to the boundary-layer growth inside the shock holder. First, if the internal-boundary-layer build-up was excessive, the shock holder became self-choking and it was impossible to draw the detached shock back into the entry plane. Some allowance for this boundary-layer growth was made by diverging the internal contour, but no very satisfactory theory exists to guide the correction, which at best would be applicable over only a very small range of flow conditions. Second, there existed certain conditions, possibly corresponding to an overcorrection for boundary layer, for which the shock would not remain stationary in the shock-holder entry but performed small random oscillations about a mean position.

Fortunately, almost every shock holder which was tried worked properly over some range of wind-tunnel conditions, so that by use of the three models shown in figure 1 it was possible to cover an adequate overall range of flows. However, even when a shock holder was operating correctly, with the shock steady in the entry plane, the internal boundary layer exerted a slight influence on the downstream tail of the shock-wave profile, as will be discussed more fully later in this report.

Normal-Shock-Wave Profiles

The normal-shock traces in raw-data form showed wire-temperature changes of about 60° F across the shock and shock thicknesses varying from a few hundredths to a few tenths of an inch. The final traces are presented in dimensionless, normalized form, as plots of t_w versus y (see "Reduction of Data"), in figures 9(a) to 9(h). Each figure shows all traces recorded at a given flow setting, including both thermocouple and resistance-wire traces and occasional repetitions of the same trace which were taken on different days or with different shock holders. The latter repetitions were frequent in the higher Mach number nozzle, because of the large amount of scatter which was encountered. For point-by-point traces with the resistance wire, the points of measurement are shown; for the continuous thermocouple traces recorded with the X-Y function plotter, the smooth curve is shown. (An exception to the last statement is seen in fig. 15(a), where points have been picked off the thermocouple trace to avoid confusion with the theoretical curve.)

Shock-Wave Thicknesses

Shock thicknesses were calculated only for those traces which were obtained with the resistance wire, since the higher Knudsen numbers obtainable with this wire gave greater assurance that the wire did not perturb the natural condition of the shock front. These results are shown in figure 12, in which δ is plotted versus the shock-strength parameter ϵ; in figure 13, in which $\mu_*/\rho u \delta_m$ is plotted versus the initial Mach number M_1; and in figure 14, in which δ_m/Λ_1 is plotted versus M_1. In all graphs the results of repeated measurements are represented by a point giving the average value and a line showing the spread of values. Various theoretical results from the literature, and experimental results by Greene, Cowan, and Hornig, are also shown in figure 13. In examining figure 13, one should note that some of the shock thicknesses shown are taken from the density profile; some, from the velocity profile; and some, from the free-molecule wire temperature profile. The effect of these inconsistencies is discussed somewhat in a later section.

Evidence of Wire-Size Effect on Shock-Wave Profile

The range of Knudsen numbers (Λ/d) encountered in the present experiments was sufficient to indicate in some instances the nature of wire-size effects when the conditions for fully developed free-molecule flow were not met. Such effects may be seen by contrasting figure 9(a), which shows identical traces obtained with a relatively large thermocouple wire $(\Lambda_*/d = 10)$ and with a much smaller resistance wire $(\Lambda_*/d = 80)$ at a flow condition for which both wires enjoy free-molecule flow, with figure 9(g), wherein the trace from the larger wire corresponds to $\Lambda_*/d = 1.3$ and that from the smaller wire corresponds to $\Lambda_*/d = 11$. Evidently the larger wire in the latter case has produced an artificial broadening of the shock front. Such comparisons between traces of identical shocks, recorded with wires of different sizes, in addition to the study of deviations between experimental and theoretical wire temperatures in the uniform stream, served to establish the Knudsen number criterion for discarding any shock traces which could contain a wire-size effect.

EXPERIMENTAL ERROR

Random Error in Measurements

The three quantities measured were two temperatures and a distance. In addition, use was made of the previously determined calibrations of the wind-tunnel jets.

The accuracy of determining the absolute level of temperature, with both thermocouples and resistance wires, was quite poor, with errors amounting to perhaps $\pm 5^{\circ}$ F. These errors remained approximately constant during a run and were mostly canceled by the method of data reduction. The sensitivity of the temperature-measuring equipment, on the other hand, was quite good, being about $\pm 0.1^{\circ}$ F for the resistance wire according to the least counts of the potentiometer and galvanometer, which corresponds to about 0.16 percent of the total change in wire temperature across a shock. The stagnation-temperature measurement also probably contained errors of a few degrees, but again the data-reduction method involves only changes in T_0 during the tracing of a shock; and these changes could be measured with a precision of about $\pm 0.3^{\circ}$ F.

Distance through the shock was measured with an effective least count of about 0.0002 inch at the higher Mach numbers (0.0001-inch-reading dial indicator) and of about 0.001 inch throughout the remainder of the tests. The smallest change in x which could be reliably measured amounted to 2 percent or less of the maximum-slope shock thickness in all cases.

Uncertainty in the calibration of the wind-tunnel jets entered into the conversion of x into y and into the specification of the initial Mach number. Previous experience with nozzles 6 and 8 indicates that there exists a probable error of ± 2 or ± 3 percent and of less than 1 percent in their respective Mach number determinations. Corresponding to this Mach number uncertainty and to the probable error of measurement in stagnation pressure and temperature, there are probable errors in l_x and Λ_1 of about ± 3 percent in nozzle 6 and of about ± 1 percent in nozzle 8. The probable error in the conversion factor y/x is considerably less, being less than 1 percent throughout, because of the fact that y/x is practically independent of M_1 within the range of nozzle 6.

The greatest source of uncertainty in the experimentally determined shock thicknesses entered through the difficulty of drawing the maximum-slope line. This error appeared to be about ± 5 percent up to about Mach number 2 and ± 10 percent at the two points around Mach number 3.8.

Systematic Experimental Error

Any new experimental method must be scrutinized carefully for sources of systematic error, and the number of possible sources of such error is great in the present experiment. It may be that the following discussion will fail to name them all, but everything which has occurred to the author individually or has been suggested by others will be given some mention, even if some items are concluded to be unimportant within the small range of tests performed so far. This discussion will be presented as an attempt to answer a number of critical questions concerning the experiment.

(a) Was the shock wave really plane and normal to the incident flow? Since both the thermocouple and the resistance wires recorded the result of an average energy balance over an appreciable length of wire, the experimental t_w traces would certainly be distorted from the true shock profile if the shock were curved in such a manner that the wire did not lie parallel to the shock front. By reason of this same averaging property, the wire itself could not be used effectively to check the planeness of the shock (for instance, by varying the position of the thermocouple junction along the length of the wire). The principal assurances that the shock was truly plane in the present tests were as follows: (1) The shock stood directly in the entry plane of the hollow shock holder, according to measurements of the wire temperature. The shock is known to be convex upstream when slightly detached, and it appears reasonable that it would be convex downstream when very slightly swallowed; the inference is that it would be plane when in the entry plane. (2) Comparison with the profiles of detached shocks from the transverse cylinder, for cases in which the detachment distance was fairly large compared with the shock thickness, showed good agreement, although what shock curvatures there could have been in the two cases were certainly very different in nature. Neither of these assurances amounts to a direct observation, and the planeness of the shock may still be open to question; in any case it is evident that the error introduced into the shock-wave profiles would be an artificial thickening.

(b) Was the shock really steady, or could it have been drifting or vibrating? High-speed schlieren photographs show that shocks in atmospheric-pressure wind tunnels frequently perform rapid oscillations about a mean position, so that shocks appear considerably sharper in high-speed photographs than in low-speed ones. At the other extreme, shocks have been observed to drift slowly in one direction in the low-density wind tunnel, in response to a transient change in the very thick boundary layer during the time a model requires to reach its equilibrium temperature in the supersonic stream. Either one of these effects, if present during the tracing of the shock profile, would raise serious questions concerning the validity of the data. Errors due to a slow drift could be avoided by waiting for the transient to pass, and considerable care was taken to do this. Vibrations, if fairly slow, would show up on the wire temperature, particularly when the wire was near the center of the shock. Such slow vibrations could be caused by mechanical vibration of the shock holder or of the choking device, or by random fluctuations in the test-chamber pressure. In either case they were easy to identify and avoid. High-frequency vibrations, on the other hand, could not be detected by the rather sluggish measuring circuits, and the only arguments against their possible existence are indirect. No one has as yet suggested any reasonable source of excitation of such high-frequency oscillations (the low-density supersonic jet is almost certainly not turbulent), and in any case the error introduced would again be a broadening of the shock front, a result which appears somewhat unlikely in view of the rather small shock thicknesses which were observed.

(c) Was the measured shock profile unduly influenced by the boundary-layer growth within the shock holder or by the geometry of the shock holder itself? During the course of preliminary and developmental experimentation it became evident that the shock was almost never followed by a long zone of perfectly uniform subsonic flow but rather by locally accelerating or decelerating flows, the exact nature of which depended upon the shock-holder geometry and the Reynolds number. Furthermore, at the lowest Reynolds numbers the effect of these nonuniform downstream boundary conditions appeared to penetrate upstream to a considerable distance through the shock wave, as evidenced by comparisons of normal shocks and detached shocks. However, final data were gathered only under conditions of minimum downstream nonuniformity; and comparisons between normal-shock traces recorded with shock holders of different sizes and shapes, or with the same shock holder at different Reynolds numbers, suggest that this effect is not very large. Nevertheless, this is one of the most real disadvantages of the present experiments and one which would merit considerable attention in an attempt to refine or extend this work.

(d) Could the t_w profile have been significantly distorted by x-dependent values of radiation and end conduction losses or of Knudsen numbers? Since the wire temperature, effective end temperature, radiant surrounding temperature, and convective-heat-transfer coefficient all changed as the wire was moved through the shock, particularly as the wire first passed the shock-holder entry plane, changing amounts of extraneous heat losses could conceivably have perturbed the shape of the shock profile. However, some direct calculations (see appendix A) and a number of indirect observations indicate that this effect was unimportant. The indirect evidence which is considered pertinent is as follows: (1) Good correlation between shock profiles at various gas pressures, for which the calculated effects of extraneous heat losses were significantly different and for which the distances of wire travel were also distinctly different; (2) lack of any discontinuity of profile slope or curvature, to be associated with the wire's passing the entry plane; and (3) good agreement between thermocouple and resistance-wire traces, end losses from the two instruments being different in calculated magnitude. Effects of varying Knudsen number may also be disregarded, since final data were retained only for traces in which the Knudsen number was everywhere above the free-molecule flow limit.

(e) Was the shock profile unduly influenced by local nonuniformity in the free-stream flow? This question has particular significance with respect to the use of an air nozzle to produce helium flows, which were not so uniform as might be desired. However, tests made with the shock holder in different axial positions (and hence in different situations regarding local nonuniformities of flow) produced essentially identical results, so that this possible source of error may apparently be dismissed.

DISCUSSION

Significance of t_w Profiles

In assessing the value of the present experimental method, one is bound to question the relative usefulness of knowing the t_w profile of a shock wave as contrasted with knowing the usual profiles such as those of velocity or temperature. This is obviously a difficult point to discuss conclusively, and the suggestions which follow cannot be expected to satisfy all critics; nevertheless, the point is too important to be passed by without mention.

There is at first the question of t_w being, for a cylinder of finite diameter, as good a point function as (say) the velocity. A theoretical argument here is difficult, since one is not frequently critical in defining how satisfactory a point function the velocity itself is; but a practical answer may be gained experimentally by observing the change in t_w which occurs when a given wire is displaced by 1 diameter across the steepest gradients in the shock. If this change is significant, then the wire is presumably too large to yield a satisfactory point measurement. (The largest such change was, at $M_1 = 3.9$, about $2\frac{1}{2}$ percent of the total change across the shock, a value which may already be excessive. The next largest was about 1 percent, at $M_1 = 3.7$, and all others were considerably less than 1 percent.)

Supposing that t_w is a satisfactory point function, one then asks how much information about the complete structure of the shock wave is gained by knowledge of the t_w profile. At the outset, it is evident from the calculations outlined in appendix B that there does not exist, except in the limit of vanishing shock strength, any inversion relation which will yield the velocity or temperature profile directly from the t_w profile. From the viewpoint of continuum theory there appear to be two reasons for this fact, the first being the general lack of locally adiabatic flow within the shock and the second being that the wire temperature is influenced by local values of the stress and heat flux in addition to the velocity and temperature. On the other hand, the calculations have shown that the t_w profile does not differ greatly from the w profile for air or helium at a Mach number up to 2, regardless of the particular theory used for the calculation. Some distinguishable differences in profile shapes for t_w and w arise from the thirteen-moment theory at a Mach number of 1.61 and from the Navier-Stokes theory for $M_1 = 3.7$, but under any circumstances it appears clear that the wire temperature is more akin to the gas velocity than to any other variable.

A more general viewpoint which is subscribed to herein is that the state of the gas at a point within the shock is determined when the molecular distribution function is known at that point and that, of all the observable mean properties (such as velocity, density, gas temperature, or free-molecule wire temperature) which can be calculated from the distribution function, no single one plays a role essentially more significant than that of any other. The function of an experiment in which only one of these observable quantities is actually measured is to infer the correctness of some theoretically postulated distribution function, in the hope that a distribution function which predicts the correct values for the measured observable quantity will also predict correctly those observable quantities which could not be measured. Thus, if it is said in this report, for example, that the Navier-Stokes equations appear satisfactory to predict the shock transition up to a Mach number of 2, what is meant is that it has been possible to find a distribution function which yields the Navier-Stokes equations when substituted into the Maxwell transport equations for mass, momentum, and energy and which, when used in the calculation of the free-molecule cylinder temperature, yields results in good agreement with experiment up to a Mach number of 2. The inference then made is that the velocity and temperature profiles which are calculated en route to the successful prediction of the t_w profile (see appendix B) are also correct.

The danger of this line of thinking lies in the obvious lack of unique correlation between a correct distribution function and a correct derived value for any single observable quantity, particularly when the range of experimental data is sharply limited, as it is in the present case. In other words, it may be possible to find two or more distinctly different distribution functions from which one could calculate practically identical t_w profiles for a shock in a given range of Mach number, whereas these same two distribution functions might lead to vastly different (say) temperature profiles for this shock. Fortunately, no such examples have appeared as a result of the theoretical calculations done so far.

The negative corollary of the above viewpoint may be a little more readily acceptable; this is, a distribution function which leads to a very poor prediction of the observed t_w profile may probably be discarded as wrong. Even this conclusion must be tempered by one's estimate of the adequacy of the technique by which the parameters of the distribution function are determined (by use of the Maxwell transport equations, etc.).

The most positive suggestion which seems appropriate for this report, in view of the presently immature condition of both the theories and experiments, is that the t_w profiles may be used to infer the general superiority of one theoretical approach over one or more alternatives and

that the free-molecule wire-temperature measurement is about as useful as a velocity or density measurement for the purpose of this inference, at least for Mach numbers up to about 2.

Comparison of Experiment With Theory

As noted in appendix B, theoretical shock profiles for comparison with experiment have been calculated for $M_1 = 1.82$ in helium, $M_1 = 1.89$ in air, and $M_1 = 3.70$ in air. The calculations were done by the Navier-Stokes and Mott-Smith methods, as indicated in table II. Figures 15(a) to 15(c) show graphical comparisons of the theoretical t_w profiles with the experimental shock traces at corresponding Mach numbers. For the helium shock, and for air at $M_1 = 1.89$, a very satisfactory fit to the data is afforded by the Navier-Stokes theory, with zero bulk viscosity in the monatomic gas and with bulk viscosity equal to about two-thirds of shear viscosity in air. The shape of the Mott-Smith profiles is satisfactory, but the shock thickness is evidently too large, at least for the ξ_x^2 transport equation (see appendix B). At $M_1 = 3.70$, none of the theories yields satisfactory agreement with the data; the Navier-Stokes profile has the wrong shape and the Mott-Smith profile is still too thick.

The thirteen-moment equations have not been solved for a normal shock wave for Mach numbers greater than 1.65, a limit which is unfortunately lower than the lowest Mach number obtained in the experiments. In order to obtain some idea as to its correctness, this theory and the Navier-Stokes theory are compared for helium at $M_1 = 1.61$ in figure 16. At this Mach number, the shape and thickness of the thirteen-moment profile are distinctly different from what would be expected from an extension of the experimental data toward lesser shock strength, assuming that good agreement between experiment and the Navier-Stokes theory continues in this region.

Relaxation Phenomena

Bulk viscosity.- The curves displayed in figure 15(b) strongly suggest that air should be characterized by a bulk viscosity coefficient as well as a shear viscosity. Although the concept of a nonzero bulk viscosity coefficient is frequently overlooked in the study of fluid dynamics, it has been the subject of many papers, both theoretical and experimental.[3]

---

[3]This literature has been very well summarized by Truesdell (ref. 36; see sec. 61A, pp. 228-231).

The conclusion to be drawn from this literature is that bulk viscosities certainly do exist in any but monatomic gases but that this fact is of little practical importance in all but a few flow situations. The exceptional circumstances are those that have been noted before: High-frequency sound absorption and dispersion, shock waves, or any flow in which the normal, rather than tangential, viscous stresses are predominant. Experimental values of bulk viscosities, as obtained from acoustical interferometry and related experiments, have been very recently collected and tabulated by Truesdell (ref. 19). The value given for air is $\kappa = 0.57\mu$, in good agreement with the value obtained by the present study of shock-wave structure.

According to several writers (e.g., Wang Chang and Uhlenbeck, ref. 37), the ratio κ/μ can be related to the relaxation time associated with the internal degrees of freedom when these degrees of freedom exchange energy "easily" with the translational degrees of freedom of the molecule (i.e., when relaxation times are small). From the relationships given in reference 37, one calculates that a bulk viscosity $\kappa = 2/3\ \mu$ implies the average requirement of 5.3 molecular encounters for the reduction of a sudden disturbance in the rotational molecular degrees of freedom, in air, to $1/e$ of its initial magnitude.

Additional relaxation effects.- Although the present findings concerning the importance of bulk viscosity in the shock wave are corroborated by the results of Greene, Cowan, and Hornig's optical-reflectivity experiments, the latter experiments seem also to have suggested some additional or residual relaxation effects downstream of the main transition zone. This has led to the feeling that the shock transition in certain diatomic and polyatomic gases may occur as a two-stage process, in which 90 percent or so of the total density change occurs relatively quickly as described by the Navier-Stokes equations with bulk viscosity, after which some final, slower adjustments are completed to bring about the final equilibrium state. Although the appearance of the wire-temperature traces would seem to deny the existence of such a two-stage shock transition in air or nitrogen, certain features of the present experiment suggest that it may be incapable of showing up the small adjustments of the second, slower stage, even if a two-stage process does exist. An interesting point is brought out by reference to appendix C and to figure 17, which suggest the possibility that the wire temperature in the downstream tail of the shock may be almost independent of the state of relaxation of the gas, particularly in the Mach number range in which most of the present data were recorded. (See particularly curves a and c in fig. 17.) While the results of appendix C are certainly inconclusive, because of the roughness of the relaxation model and the lack of knowledge of values for the various accommodation coefficients, there are two other features of the present work, namely, the limited experimental accuracy and the distortion of the downstream tail of the shock by boundary-layer growth in the shock holder, which would definitely hinder detection of a second stage in the

shock transition. Therefore, one may conclude that the wire-temperature traces do not suggest any sort of two-stage shock wave, but neither do they preclude the possibility of its existence.

Comparison of wire-temperature data with optical-reflectivity data.- As may be seen in figure 13, there was unfortunately little Mach number overlap between the wire-temperature data and the data of Greene, Cowan, and Hornig, and where the overlap occurred, at about $M_1 = 2$, the two types of experimental shock thickness are in rather poor agreement. However, of the optical-reflectivity data, only the relatively isolated points at $M_1 = 2.1$ differ very significantly from the Navier-Stokes predictions. The rest of these data may be fitted quite satisfactorily by Navier-Stokes theories, with bulk viscosity equal to zero for the monatomic gas and with a bulk viscosity, for the diatomic gases, approximately equal to the value used to fit the wire-temperature data for air and nitrogen. Because of the extreme difference in the experimental methods, this implied agreement between the present results and those obtained by Greene, Cowan, and Hornig seems quite remarkable.

CONCLUDING REMARKS

The profiles and thicknesses of normal shock waves of moderate strength have been determined experimentally in terms of the variation of the equilibrium temperature of an insulated transverse cylinder in free-molecule flow. The shock waves were produced in a steady state in the jet of a low-density wind tunnel, at initial Mach numbers of 1.72 and 1.82 in helium and 1.78, 1.85, 1.90, 1.98, 3.70, and 3.91 in air. The shock thickness, determined from the maximum slope of the cylinder temperature profile, varied from 5 to $3\frac{1}{2}$ times the length of the Maxwell mean free path in the supersonic stream. A comparison between the experimental shock profiles and various theoretical predictions leads to the tentative conclusions that: (1) The Navier-Stokes equations are adequate for the description of the shock transition for initial Mach numbers up to 2, and (2) the effects of rotational relaxation times in air can be accounted for by the introduction of a "second" or "bulk" viscosity coefficient equal to about two-thirds of the ordinary shear viscosity.

University of California,
Berkeley, Calif., May 24, 1954.

APPENDIX A

NUMERICAL EVALUATION OF CONDUCTION AND RADIATION LOSSES FROM EQUILIBRIUM-TEMPERATURE CYLINDER

A very comprehensive study of the effects of conduction and radiation heat losses on the temperature of a bare thermocouple or resistance thermometer in contact with a gas has been given in reference 38. This has been used, in conjunction with empirical information supplied by the authors of reference 29, to estimate the severity of these effects in the present experiments.

To begin with, the observation made by the authors of reference 29 in experiments involving the free-molecule cylinder in a uniform stream was that radiation losses from all wires tested were practically negligible but that end losses from their models were serious. The first conclusion agrees nicely with information on the radiant emissivities of iron and tungsten (ref. 39), giving them to be all about 0.1. This may be seen by evaluating the relative magnitudes of the radiation and convection terms in the full heat-balance equation (ref. 29):

$$(j + 4)f(s)\frac{T_w}{T} = a(s) - \frac{4\pi^{3/2}}{pV_m\alpha}\left[\epsilon\sigma\left(T_w^4 - T_s^4\right)\right] \qquad (A1)$$

As the worst conditions encountered in the present tests, take

$j = 2$ (in $a(s)$, as in eqs. (B24))

$s = 1.4$

$p = 38\ \mu$ Hg $= 0.106$ lb/sq ft (static pressure)

$V_m = 1{,}074$ ft/sec (most probable molecular speed)

$\alpha = 0.9$ (accommodation coefficient)(refs. 29 and 40)

$\epsilon = 0.1$ (radiant emissivity)

$T_w = 598^\circ$ R

$T_s = 523^\circ$ R (temperature of radiant surroundings)

$\sigma = 3.74 \times 10^{-10}$ ft-lb/(sq ft)$(^\circ R)^4$(sec)(Stefan-Boltzmann constant)

The first term on the right of equation (A1) represents convection and has the magnitude 60.2. The second or radiation term has the magnitude 0.44, thus causing a 0.7 percent or about 4.3° F drop in T_w.

It is interesting to make a companion calculation of the radiation loss downstream of a normal shock wave at this same flow setting. There,

$$s = 0.536$$

$$p = 0.340 \text{ lb/sq ft}$$

$$V_m = 1,296 \text{ ft/sec}$$

$$T_w = 554^{\circ} \text{ R}$$

(All other quantities are the same as in the above example.) In this case the convective term has the magnitude 24.3, and the radiant term amounts to 0.040, causing a 0.17 percent or 0.9° F drop in T_w. It is seen that in this worst case radiation losses can have a measurable but unimportant effect on the shock profile.

In order to evaluate the effects of end conduction losses on the temperature distribution along the cylinder, an approximate value of the heat-transfer coefficient due to free-molecule convection is needed first. This is given in reference 29 in a form equivalent to

$$h_c = \frac{j + 4}{4\pi^{3/2}} f(s) \frac{pV_m\alpha}{T} \qquad (A2)$$

This reaches its minimum value, within the present experimental range, at the flow setting cited above. Ahead of the shock, where $T = 336^{\circ}$ R, its value is

$$h_c = \frac{(0.106)(1,074)(0.9)(16.96)}{(11.12)(336)}$$

$$= 0.466 \text{ ft-lb/(sq ft)(sec)}(^{\circ}\text{R})$$

$$= 2.2 \text{ Btu/(sq ft)(hr)}(^{\circ}\text{R})$$

Downstream of the shock, where $T = 490^{\circ}$ R,

$$h_c = \frac{(0.340)(1,296)(0.9)(10.72)}{(11.12)(490)} \frac{3,600}{778}$$

$$= 3.6 \text{ Btu/(sq ft)(hr)}(^{\circ}\text{R})$$

To continue with the end-loss calculation, two formulas are now drawn from reference 38. Both deal with the temperature distribution in a cylinder of length $2L$, whose ends are in perfect thermal contact with infinite heat reservoirs at temperature T_e and which exchanges heat with a surrounding gas, the heat-transfer coefficient being constant along the wire length. Introduce the symbols

h	heat-transfer coefficient to gas
K	thermal conductivity of cylinder
d	cylinder diameter
T_w	equilibrium temperature of cylinder
T_w'	equilibrium temperature of cylinder in absence of end conduction losses

and

$$m = \sqrt{\frac{4h}{dK}}$$

The first formula gives the center-point temperature of a butt-welded thermocouple made of wires of the same diameter but of different conductivities. Let the subscripts 1 and 2 distinguish between properties of the two wires, but assume h to be the same for both. Then

$$\frac{T_w - T_w'}{T_e - T_w'} = \frac{2K_1m_1 \sinh\left(m_2L\right) + 2K_2m_2 \sinh\left(m_1L\right)}{\left(K_1m_1 + K_2m_2\right) \sinh\left[\left(m_1 + m_2\right)L\right] - \left(K_1m_1 - K_2m_2\right) \sinh\left[\left(m_1 - m_2\right)L\right]} \tag{A3}$$

This relation is plotted versus m_1L in figure 18 for the interesting case where material 1 is iron and material 2 is constantan. For this purpose the conductivity of iron was taken to be exactly three times that of constantan.

The second formula gives the average temperature of the centrally located fraction $2bL$ of the total length of a monometallic wire,

$$\frac{T_w - T_{w'}}{T_e - T_{w'}} = \frac{\tanh (mL) \cosh \left[m(1 - b)L\right] - \sinh \left[m(1 - b)L\right]}{bmL} \tag{A4}$$

which is plotted versus mL in figure 18 for the case $b = 0.3$. Shown for comparison is the case for $b = 0$, which simply gives the center-point temperature of the wire.

A pair of conservative numerical examples will now be worked out, for consideration of the present data, using dimensions and properties of the actual thermocouples and resistance wires. Clearly, the end-loss effect will be greatest when the convective-heat-transfer coefficient is smallest, so the previously calculated minimum value $h = 2.2$ is used. Proceeding first to the case of an iron-constantan thermocouple 0.002 inch in diameter, the following values are used:

$$K(\text{iron}) = 35 \text{ Btu/(hr)(ft)(}^\circ\text{R)}$$

$$h = 2.2 \text{ Btu/(hr)(sq ft)(}^\circ\text{R)}$$

$$d = 1.67 \times 10^{-4} \text{ ft}$$

So

$$m(\text{iron}) = \frac{(4)(2.2)}{(35)(1.67)} \times 10^2 = 38.8$$

The choice of values for L and for T_e is less straightforward, for several reasons. The actual physical length of the wires was about 5 inches, but the length along which the flow properties and heat-transfer coefficient were constant was only about 1.5 inches. Whereas the temperature at the ends of the 5-inch length is probably very close to the temperature of the wind-tunnel shell, it is very hard to guess an effective end temperature to apply at the ends of the length along which the uniform properties prevail. Traverses made with a short thermocouple probe such as is shown in figure 5 have demonstrated that the equilibrium temperature first rises as the probe moves from the free stream into the supersonic edge of the boundary layer and then drops rapidly

to a value close to the recovery temperature of the nozzle wall as the remainder of the boundary layer is crossed. Since the only purpose in the present analysis is to see whether end conduction losses are important, an arbitrary and presumably pessimistic choice will be made as follows:

$$L = 3/4 \text{ in.} = 0.0625 \text{ ft}$$

$$T_e - T_{w'} = -30^\circ \text{ R}$$

$$mL = 2.42$$

and from figure 18

$$\frac{T_w - T_{w'}}{T_e - T_{w'}} = 0.12$$

so that

$$T_w - T_{w'} = 3.6^\circ \text{ R}$$

The second calculation will be done for the same flow conditions and the same guess as to the effective length and end temperature but now for a resistance-wire thermometer with $b = 0.3$, $d = 2.08 \times 10^{-5}$ foot, and $K = 87$ Btu/(hr)(ft)($^\circ$R). With these values, one may calculate

$$mL = 0.0625\sqrt{\frac{(4)(2.2)}{(87)(0.0000208)}} = 4.4$$

From figure 18 there is obtained

$$\frac{T_w - T_{w'}}{T_e - T_{w'}} = 0.03$$

so that the end effect is just about one quarter of that noted for the thermocouple. To be conservative, this is doubled to allow for the extra losses down the potential leads.

In the case of the resistance wire, which necessarily carries a small current, there is also a possible extraneous effect on the equilibrium temperature due to the electrical heating. This may be evaluated

by use of equation (B23) of reference 28, which gives the corresponding term in the energy equation to be

$$-\frac{4\pi^{3/2}}{pV_m\alpha}Q$$

where

$$Q = \frac{i^2R}{\pi dL}$$

R being the resistance of the wire length L. For the present case,

$$i = 2 \times 10^{-4} \text{ amp}$$

$$R = 27 \text{ ohms}$$

$$d = 2.08 \times 10^{-5} \text{ ft}$$

$$L = 0.042 \text{ ft}$$

yielding

$$Q = 0.39 \text{ watt/sq ft} = 0.29 \text{ ft-lb/(sec)(sq ft)}$$

By comparison with the first calculations of this section, concerning radiation losses, it is seen that this effect opposes that of radiation and amounts to about one-seventh and two-fifths of the latter before and behind the shock, respectively.

APPENDIX B

THEORETICAL CALCULATIONS OF WIRE TEMPERATURE PROFILES

Since the only known method of calculating the equilibrium temperature of the free-molecule cylinder involves direct use of the molecular distribution function, the first step in the prediction of the wire temperature profile of a shock is the calculation of the distribution function at each point within the shock. The methods by which this step is taken are either selected from general attacks on the theory of nonuniform gases, such as the Enskog-Chapman method or the thirteen-moment method, or specially formulated to describe the shock-wave transition, as in the method of Mott-Smith. The starting point is unanimously taken to be the Boltzmann integrodifferential equation, which equates the rates of change in the distribution function due to the processes of drift and collision. Each separate method assumes the distribution function in a more or less distinct form, in which some of the observable properties of the mean gas motion appear as parameters and which is capable of assuming the form for Maxwellian equilibrium with streaming velocity when the observable properties take on their values appropriate to the uniform flows upstream and downstream of the shock. This assumed distribution function is then substituted into the Maxwell transport equations for the summational invariants of an intermolecular collision (mass, momentum, and total molecular energy), and possibly for various other quantities as needed, to provide a set of equations which can be solved subject to the shock-wave boundary conditions to yield the spatial distribution of the observable parameters of the distribution function. (This description is historically incorrect in the case of the Enskog-Chapman method but is adequate for the present task.) These equations in mean quantities are simply the Navier-Stokes, Burnett, or thirteen-moment equations which have served as the starting point for many theoretical papers on shock-wave structure or, in the Mott-Smith calculations, they amount simply to the Rankine-Hugoniot equations relating the shock-wave end conditions, plus one specialized transport equation.

Enskog-Chapman Method, Navier-Stokes Approximation

For the calculation using the Enskog-Chapman method, the distribution function is taken in a form capable of describing both monatomic gases and a limited class of diatomic gases for which the exchange of energy between the translational and internal degrees of freedom of the molecule is easy. This form of the distribution function was suggested by reference 37:

$$f_i = n\left(\frac{m}{2\pi kT}\right)^{3/2} \frac{1}{\sum_s e^{-E_s/kT}} e^{-\frac{1}{kT}\left(\frac{mC^2}{2}+E_i\right)}\left[1 - \right.$$

$$\mu\left(\frac{\partial u_\alpha}{\partial r_\beta} + \frac{\partial u_\beta}{\partial r_\alpha} - \frac{2}{3}\delta_{\alpha\beta}\frac{\partial u_\gamma}{\partial r_\gamma}\right)\frac{mC_\alpha C_\beta}{2nk^2T^2} - \frac{\kappa}{nkT}\frac{\partial u_\gamma}{\partial r_\gamma}\left(\frac{mC^2}{2kT} - \frac{3E_i}{jkT}\right) -$$

$$\left.\lambda^{tr}\frac{\partial T}{\partial r_\alpha}\frac{mC_\alpha}{nk^2T^2}\left(\frac{mC^2}{5kT} - 1\right) - \lambda^{int}\frac{\partial T}{\partial r_\alpha}\frac{mC_\alpha}{nk^2T^2}\left(\frac{2E_i}{jkT} - 1\right)\right] \qquad (B1)$$

The mean flow properties which appear as parameters in this expression are n, $\vec{u}$, and T. The number density of molecules in coordinate space n and the mean flow velocity $\vec{u}$ are defined in the usual way by the following averages over the distribution function:

$$n = \sum_i \iiint_{-\infty}^{\infty} \vec{d\xi}\, f_i\left(\vec{\xi},\vec{r},E_i\right)$$

$$u_\alpha = \frac{1}{n}\sum_i \iiint_{-\infty}^{\infty} \vec{d\xi}\, \xi_\alpha f_i\left(\vec{\xi},\vec{r},E_i\right)$$

The temperature T is proportional to the mean total random molecular energy and is given by the expression

$$T = \frac{2}{(j+3)nk}\sum_i \iiint_{-\infty}^{\infty} \vec{d\xi}\left(\frac{1}{2}mC^2 + E_i\right) f_i\left(\vec{\xi},\vec{r},E_i\right)$$

The mean flow velocity enters the distribution function both explicitly, in the terms of the form $\partial u_\alpha/\partial u_\beta$, and implicitly, in the quantity C^2, since

$$\left.\begin{aligned} \vec{C} &= \vec{\xi} - \vec{u} \\ C^2 &= \left(\xi_x - u_x\right)^2 + \left(\xi_y - u_y\right)^2 + \left(\xi_z - u_z\right)^2 \end{aligned}\right\} \tag{B2}$$

where $\vec{\xi}$ is the total absolute velocity of a molecule, $\vec{C}$ is the random "thermal agitation" velocity, and ξ_x, ξ_y, and ξ_z are the Cartesian components of the vector $\vec{\xi}$.

The distribution function, as written above, purports to give the number density, in a $6 + j$ dimensional phase space, of molecules having position between $\vec{r}$ and $\vec{r} + \vec{dr}$, velocity between $\vec{\xi}$ and $\vec{\xi} + \vec{d\xi}$, and internal energy between E_i and $E_i + dE_i$, the internal energy being the result of molecular rotations or vibrations. Since the present experiments are concerned primarily with well-excited molecular rotations as a source of internal energy, attention has been restricted to a molecular model whose internal energy may be assumed to be of quadratic form in some continuous variable having the range $-\infty$ to ∞ in j degrees of freedom. It has been assumed, furthermore, that the translational and internal motions of the molecule are independent, so that integrations over translational velocities and over internal energies may be freely interchanged in order. The assumption of the form of the internal energy allows the summations over internal-energy states to be replaced by integrations and leads to the following useful formulas:

$$\left.\begin{aligned} \frac{\sum_i \epsilon_i e^{-\epsilon_i}}{\sum_i e^{-\epsilon_i}} &= \frac{j}{2} \\ \frac{\sum_i \epsilon_i^2 e^{-\epsilon_i}}{\sum_i e^{-\epsilon_i}} &= \frac{j}{4}(j+2) \end{aligned}\right\} \tag{B3}$$

where

$$\epsilon_i = \frac{E_i}{kT}$$

The distribution function (B1) contains other symbols and some notations which have not been used previously in this report and which are consequently listed below:

k	Boltzmann constant
m	mass of a molecule
μ	coefficient of shear viscosity
κ	coefficient of bulk viscosity
λ^{tr}	heat-conduction coefficient for random translational energy
λ^{int}	heat-conduction coefficient for random internal energy
α,β,γ	tensor indices, used with convention of summation over repeated indices
$\delta_{\alpha\beta}$	Kronecker delta function; 1 when $\alpha = \beta$ and 0 when $\alpha \neq \beta$

The first step in the theoretical prediction of the wire temperature profile of a shock wave, the determination of the spatial variation of the parameters n, $\vec{u}$, and T, is taken by substituting expression (B1) into the Maxwell transport equations (refs. 17 and 18) for the quantities $\vec{m}$, $m\xi$, and $\frac{1}{2}m\xi^2 + E_i$, where $\xi^2 = \xi_x^2 + \xi_y^2 + \xi_z^2$. All integrations and summations may be easily performed, and the procedure yields the familiar conservation equations known as the Navier-Stokes equations for a compressible, viscous, heat-conducting gas. These equations are specialized here for the case of a one-dimensional, steady flow:

$$\left.\begin{aligned}
&\frac{d}{dx}(nmu) = 0 \\
&\frac{d}{dx}\left[nmu^2 + nkT - \left(\frac{4}{3}\mu + \kappa\right)\frac{du}{dx}\right] = 0 \\
&\frac{d}{dx}\left\{nmu\left(\frac{j+3}{2}\frac{kT}{m} + \frac{1}{2}u^2\right) + u\left[nkT - \left(\frac{4}{3}\mu + \kappa\right)\frac{du}{dx}\right] - \lambda\frac{dT}{dx}\right\} = 0
\end{aligned}\right\} \quad (B4)$$

in which $\lambda = \lambda^{int} + \lambda^{tr}$ = Total heat conductivity.

Each of these equations may be integrated once immediately, yielding, with some regrouping of terms in the third equation,

$$\left.\begin{aligned}
&nmu = M \\
&nmu^2 + nkT - \left(\frac{4}{3}\mu + \kappa\right)\frac{du}{dx} = P \\
&\frac{1}{2}nmu^3 + \frac{1}{2}(j+5)unkT - \left(\frac{4}{3}\mu + \kappa\right)u\frac{du}{dx} - \lambda\frac{dT}{dx} = \frac{Q}{2}
\end{aligned}\right\} \quad (B5)$$

Here M, P, and Q are constants of the flow (note that this M is not the Mach number), which will be used in forming the following list of dimensionless variables (ref. 15):

$$\left.\begin{aligned}
v &= Mu/P \\
\tau &= M^2kT/P^2m \\
r &= nmP/M^2 \\
\alpha &= MQ/P^2
\end{aligned}\right\} \quad (B6)$$

and the two reference lengths

$$\left.\begin{aligned}
L &= \frac{1}{M}\left(\mu + \frac{3}{4}\kappa\right) \\
L' &= \frac{4}{15}\frac{\lambda m}{kM}
\end{aligned}\right\} \quad (B7)$$

In terms of these variables, equations (B5) may be written as

$$\left.\begin{aligned} rv &= 1 \\ rv^2 + r\tau - \frac{4}{3} L \frac{dv}{dx} &= 1 \\ rv^3 + (j + 5)r\tau v - \frac{8}{3} Lv \frac{dv}{dx} - \frac{15}{2} L' \frac{d\tau}{dx} &= \alpha \end{aligned}\right\} \tag{B8}$$

The first of these may be used to eliminate r in the other two, which, when rearranged slightly, may be written as

$$\left.\begin{aligned} \frac{4}{3} L \frac{dv}{dx} &= v + \frac{\tau}{v} - 1 \\ \frac{15}{2} L' \frac{d\tau}{dx} &= 2v - v^2 + (j + 3)\tau - \alpha \end{aligned}\right\} \tag{B9}$$

The boundary conditions subject to which equations (B9) must be solved for a shock wave are

$$\frac{dv}{dx} = \frac{d\tau}{dx} = 0 \quad \text{at} \quad x = \pm\infty \tag{B10}$$

Imposition of conditions (B10) upon equations (B9) yields simple simultaneous algebraic equations which may be solved to display the Rankine-Hugoniot equations in terms of the present variables. The results are

$$\left.\begin{aligned} v = \frac{1}{r} &= \frac{1}{2(j + 4)}\left[(j + 5) \pm \epsilon\right] \\ \tau &= \frac{1}{4(j + 4)^2}\left[\left(j^2 + 8j + 15\right) \mp 2\epsilon - \epsilon^2\right] \end{aligned}\right\} \tag{B11}$$

in which the upper sign pertains to the upstream limit and the lower sign, to the downstream limit, and in which there appears a new shock-strength parameter

$$\epsilon = \sqrt{(j + 5)^2 - 4(j + 4)\alpha} \tag{B12}$$

which is related to the initial Mach number by

$$\left.\begin{aligned} M_1^2 &= \left(\frac{j + 3}{j + 5}\right)\left(\frac{j + 5 + \epsilon}{j + 3 - \epsilon}\right) \\ \epsilon &= \frac{\left(j^2 + 8j + 15\right)\left(M_1^2 - 1\right)}{(j + 3) + (j + 5)M_1^2} \end{aligned}\right\} \tag{B13}$$

The methods of reference 15 will be continued here with the introduction of normalized velocity and temperature variables w and t, which run from 1 to -1 and from -1 to 1, respectively, as the shock is traversed from upstream to downstream. These new variables are defined by the equations

$$\left.\begin{aligned} v &= \frac{1}{2(j + 4)}\left[(j + 5) + \epsilon w\right] \\ \tau &= \frac{1}{4(j + 4)^2}\left[\left(j^2 + 8j + 15\right) - \epsilon^2 + 2\epsilon t\right] \end{aligned}\right\} \tag{B14}$$

If equations (B9) are rewritten in terms of the normalized variables, and if the second equation is then divided by the first, the distance variable x is eliminated and the direction field equation for the velocity-temperature integral is obtained in the form

$$\frac{dt}{dw} = \vartheta\,\frac{\left[2(j + 3)(t + w) + \epsilon\left(1 - w^2\right)\right]\left[(j + 5) + \epsilon w\right]}{2(t + w) - \epsilon\left(1 - w^2\right)} \tag{B15}$$

in which the dimensionless parameter ϑ is proportional to the Prandtl number by

$$\vartheta = \frac{4}{45}\frac{L}{L'}$$

$$= \frac{1}{3}\left(1 + \frac{3\kappa}{4\mu}\right)\frac{\mu k}{\lambda m}$$

$$= \frac{1}{3}\left(1 + \frac{3\kappa}{4\mu}\right)\left(\frac{2}{j + 5}\right)\frac{\mu c_p}{\lambda}$$

or

$$\vartheta = \frac{1}{3}\left(1 + \frac{3\kappa}{4\mu}\right)\left(\frac{2}{j + 5}\right)\mathrm{Pr} \tag{B16}$$

For the purpose of the present calculations, equation (B15) may be integrated numerically, with the saddle-point singularity (refs. 15 and 16) $w = -1$, $t = 1$ as initial point and with initial slope determined from equation (B15) by L'Hospital's rule. For the particular integrations which were carried out, it appeared entirely satisfactory to take increments of $\Delta w = 0.1$, with an occasional need for finer steps as the upstream limit was approached. The Prandtl number was usually considered constant throughout the shock, although no essential difficulty and little additional work is involved in using the empirical variation of Prandtl number with temperature for the particular gas concerned.

Having found t as a function of w within the shock, w may now be calculated as a function of x by a second numerical integration, this time of the momentum equation (first of eqs. (B9)), which now takes the form

$$\frac{4}{3} L \frac{dw}{dx} = \frac{2(t + w) - \epsilon(1 - w^2)}{(j + 5) + \epsilon w} \tag{B17}$$

Before this is done, it is interesting to introduce a dimensionless distance variable y, defined by

$$y = \left(\frac{j + 4}{j + 5}\right)\frac{\left(\frac{3\kappa}{4\mu} + 1\right)\mathrm{Pr}}{2 + (j + 3)\left(\frac{\kappa}{\mu} + \frac{4}{3}\right)\mathrm{Pr}}\frac{\epsilon x}{L_*} \tag{B18}$$

in which the reference length L_* is to be evaluated at a temperature T_* which has here been chosen as

$$T_* = \frac{j + 3}{j + 4} T_o \tag{B19}$$

T_o being the reservoir temperature associated with the uniform flow at either end of the shock. This choice is entirely arbitrary and is considered appropriate to the present investigation because this value of the temperature is reached at or near the point of maximum shear stress and because it is very nearly a constant for each gas tested in the wind tunnel, which operates at essentially constant T_o.

The choice of y as a dimensionless distance is such that the limiting profile for a shock of zero strength has a particularly simple form in terms of w and y. The form is independent of j, Pr, the temperature dependence of viscosity, the particular dependent variable (i.e., velocity, temperature, or density), and the scheme of calculation (i.e., Navier-Stokes or thirteen-moment) and is equivalent to Taylor's early solution for the profile of a vanishingly weak shock. Thus, as ϵ tends toward zero, the shock profile becomes

$$y = \frac{1}{2} \log_e\left(\frac{1 - w}{1 + w}\right) \tag{B20}$$

As a final step previous to the next integration, equation (B17) may be rewritten in the form

$$dy = \left(\frac{j + 4}{j + 5}\right) \frac{\left(\frac{\kappa}{\mu} + \frac{4}{3}\right)\mathrm{Pr}}{2 + (j + 3)\left(\frac{\kappa}{\mu} + \frac{4}{3}\right)\mathrm{Pr}} \epsilon \frac{L}{L_*} \frac{(j + 5) + \epsilon w}{2(t + w) - \epsilon\left(1 - w^2\right)} dw \tag{B21}$$

The ratio $L/L_* = \mu/\mu_*$ may be calculated from tabulated viscosity data for the gas and temperatures involved, or it may be approximated by some simple empirical fitting formula such as the power law

$$\frac{L}{L_*} = \left(\frac{T}{T_*}\right)^{\omega} \tag{B22}$$

The choice of zero point for y is entirely arbitrary; in the present calculations y was usually taken to be zero in the vicinity of the maximum dw/dy, and the numerical integration proceeded upstream and downstream from that point by use of the trapezoidal rule, which seemed sufficiently accurate for this application.

The spatial variation of the parameters of the distribution function having thus been found, the calculation of the equilibrium temperature of the free-molecule cylinder proceeds by direct application and extension of the analysis of reference 30. The distribution function used here is somewhat different from that employed in reference 30, but the arguments and analysis are identical and will not be repeated here. The final equation for the steady-state energy balance on an insulated cylinder, with equal accommodation of translational and internal molecular energies to the temperature of the wire, can be put in the form

$$(j+4)\frac{T_w}{T} = \frac{a(s) + b(s)\left(\frac{4}{3}\frac{\mu}{nkT}\frac{du}{dx}\right) + c(s)\left(\frac{\kappa}{nkT}\frac{du}{dx}\right) + d(s)\left(\frac{\lambda^{tr}}{nukT}\frac{dT}{dx}\right) + e(s)\left(\frac{\lambda^{int}}{nukT}\frac{dT}{dx}\right)}{f(s) + g(s)\left(\frac{4}{3}\frac{\mu}{nkT}\frac{du}{dx}\right) + h(s)\left(\frac{\kappa}{nkT}\frac{du}{dx}\right) + i(s)\left(\frac{\lambda^{tr}}{nukT}\frac{dT}{dx}\right) + 0} \tag{B23}$$

The new variables which appear are T_w, the wire temperature, and s, the molecular speed ratio. The coefficient functions are:

$$\left.\begin{aligned}
a(s) &= \left[2s^4 + (j+7)s^2 + j + 4\right]I_0 + \left[2s^4 + (j+5)s^2\right]I_1 \\
b(s) &= \frac{1}{8}\left\{\left[14s^2 + (j+6)\right]I_0 + \left[14s^2 - (3j+12)\right]I_1\right\} \\
c(s) &= \frac{1}{2}\left\{\left[5s^2 + (j+6)\right]I_0 + 5s^2 I_1\right\} \\
d(s) &= \frac{1}{5}\left[(10-j)s^2 I_0 + (j+12)I_1\right] \\
e(s) &= \frac{1}{5}\left(10s^2 I_0 + 10s^2 I_1\right) \\
f(s) &= \left(s^2+1\right)I_0 + s^2 I_1 \\
g(s) &= \frac{1}{8}\left(I_0 - 3I_1\right) \\
h(s) &= \frac{1}{2}I_0 \\
i(s) &= \frac{1}{5}\left(s^2 I_0 - s^2 I_1\right)
\end{aligned}\right\} \tag{B24}$$

where

$$I_o = I_o\left(\frac{s^2}{2}\right)$$

$$I_1 = I_1\left(\frac{s^2}{2}\right)$$

are the modified Bessel functions of the first kind, of zeroth and first orders. The speed ratio s is known at each point in the shock, being defined by

$$s = v/\sqrt{2\tau} \tag{B25}$$

Equation (B23) suffices for the calculation of the wire temperature profile of the shock, since all quantities except T_w are known. For purposes of comparison with the velocity profile, or with experimental wire temperature profiles, T_w is made dimensionless and is normalized to run from 1 to -1 by the definition

$$t_w = 2\,\frac{T_w - T_{w_2}}{T_{w_1} - T_{w_2}} - 1 \tag{B26}$$

The subscripts 1 and 2 refer to upstream and downstream limit values here, as throughout the rest of this report.

This completes the prediction of the wire temperature profile of a normal shock wave, according to the Navier-Stokes equations. Curves of w and of t_w versus y have been calculated for a number of conditions, as noted in table II.

It may be interesting to note some numerical magnitudes of the contributions to the wire temperature due to the non-Maxwellian terms of the distribution function. For this purpose, use may be made of the approximate formula

$$\frac{T_w}{T_w{}^o} \approx 1 + K_1(s)\,\frac{p_{xx}}{nkT} + K_2(s)\,\frac{q_x}{nkTu}$$

where $T_w{}^o$ is the wire temperature in a gas with Maxwellian distribution function and K_1 and K_2 are complicated functions of the speed ratio s. The second and third terms on the right are the fractional contributions to the wire temperature due, respectively, to stress and heat

flux. These terms reach a maximum absolute value in the vicinity of the center of the shock, at which point a few typical values are as follows:

For helium at $M_1 = 1.61$ (Navier-Stokes):

$$\left[K_1(s)\,\frac{p_{xx}}{nkT}\right]_{max} = 0.021$$

$$\left[K_2(s)\,\frac{q_x}{nkTu}\right]_{max} = -0.036$$

For helium at $M_1 = 1.82$ (Navier-Stokes):

$$\left[K_1(s)\,\frac{p_{xx}}{nkT}\right]_{max} = 0.032$$

$$\left[K_2(s)\,\frac{q_x}{nkTu}\right]_{max} = -0.054$$

For air at $M_1 = 1.89$ $\left(\text{Navier-Stokes}, \quad \kappa = \frac{2}{3}\,\mu\right)$:

$$\left[K_1(s)\,\frac{p_{xx}}{nkT}\right]_{max} = 0.041$$

$$\left[K_2(s)\,\frac{q_x}{nkTu}\right]_{max} = -0.036$$

For air at $M_1 = 3.68$ $\left(\text{Navier-Stokes}, \quad \kappa = \frac{2}{3}\,\mu\right)$:

$$\left[K_1(s)\,\frac{p_{xx}}{nkT}\right]_{max} = 0.139$$

$$\left[K_2(s)\,\frac{q_x}{nkTu}\right]_{max} = -0.137$$

Evidently the effects of stress p_{xx} and heat flux q_x are mutually opposing, so that the combined effect upon the wire temperature frequently understates the significance of the individual terms.

It is interesting to note the necessity for guessing a value of λ^{int}/λ for air in order to calculate the t_w profile, whereas no such need arose in the calculation of the velocity profile. This occurs because the total heat flux enters the energy equation for the gas alone, while the fluxes of random translational and internal molecular energies play quite separate roles in the energy exchange between the gas and the cylinder. The guess made is entirely an uninformed one and amounts to taking the heat-conduction coefficients λ^{tr} and λ^{int} in the same proportion as the average random energy contents $3kT/2$ and jkT. It is fortunate that the calculated value of t_w is not very sensitive to the exact ratio of the conductivities.

Another interesting observation drawn from these calculations is that, up to a Mach number of 2, the dominant terms in equation (B23) are $a(s)$ and $f(s)$, the terms which would result if the wire-temperature calculation were based simply upon a distribution function of Maxwellian form with parameters $n(x)$ and $T(x)$, whose spatial variation is determined by the Navier-Stokes equations. The contributions of the terms involving velocity and temperature gradients in equation (B23) become increasingly important as the shock strength increases and are definitely significant within the Mach number range covered experimentally.

Thirteen-Moment Method

The distribution function is written in the form (ref. 18)

$$f = n\left(\frac{m}{2\pi kT}\right)^{3/2} e^{-mC^2/2kT}\left[1 + \frac{p_{\alpha\beta}}{2p}\frac{mC_\alpha C_\beta}{kT} + \frac{q_\alpha}{p}\frac{mC_\alpha}{kT}\left(\frac{mC^2}{5kT} - 1\right)\right] \qquad (B27)$$

The additional parameters which distinguish this expression from the corresponding one in the Enskog-Chapman formulation are $p_{\alpha\beta}$, the divergenceless part of the stress tensor, and q_α, the heat-flux-vector component. These new variables are considered to be independent, rather than expressible in terms of velocity and temperature gradients, and their presence requires two extra equations in addition to those expressing conservation of mass, momentum, and energy. These extra equations are obtained from the Maxwell transport equations for the quantities $C_\alpha C_\beta$ and $C_\alpha C^2$ by the methods described in reference 18. The symbol p is

introduced as an abbreviation for nkT and may be identified with the thermodynamic pressure and the mean normal stress at a point, since this entire representation is intended only for a monatomic gas.

The prediction of the normal-shock velocity and temperature profiles by the thirteen-moment method has been carried through in reference 15, so that the analysis need not be repeated here. The only difference between Grad's calculations and those done for the present report lies in a slightly different choice for the reference temperature T_*.

The calculation of the wire equilibrium temperature follows the same lines as in the last section, being in this case quite identical to the analysis of reference 30. The steady-state energy-balance equation analogous to equation (B23) is

$$4\frac{T_w}{T} = \frac{a(s) + b(s)\frac{p_{xx}}{p} + d(s)\frac{q_x}{pu}}{f(s) + g(s)\frac{p_{xx}}{p} + i(s)\frac{q_x}{pu}} \tag{B28}$$

The coefficient functions $a(s)$, $b(s)$, and so forth are the same as those listed in equations (B24) for the case $j = 0$.

This method was used to calculate the t_w and w profiles of just one shock wave, for helium at $M_1 = 1.61$, $\epsilon = 1.5$, $Pr = 2/3$, and $\mu \propto T^{0.663}$. The comparison with the corresponding Navier-Stokes prediction is shown in figure 16.

Mott-Smith Method

According to the Mott-Smith method, the gas within the shock is imagined to be a mixture of two families of molecules, one having the mean velocity and temperature of the gas upstream of the shock and the other having the mean velocity and temperature of the gas downstream. The proportions of the mixture are allowed to vary with distance through the shock, in a manner satisfying the shock-wave boundary conditions plus a rather arbitrarily chosen transport equation. The distribution function is written as

$$f = n_1(x)\left(\frac{m}{2\pi kT_1}\right)^{3/2} e^{-\frac{m}{2kT_1}\left[\left(\xi_x-u_1\right)^2+\xi_y{}^2+\xi_z{}^2\right]} +$$

$$n_2(x)\left(\frac{m}{2\pi kT_2}\right)^{3/2} e^{-\frac{m}{2kT_2}\left[\left(\xi_x-u_2\right)^2+\xi_y{}^2+\xi_z{}^2\right]} \qquad \text{(B29)}$$

The method used to determine $n_1(x)$ and $n_2(x)$ is amply described in reference 13. Substitution of distribution function (B29) into the Maxwell transport equations for mass, momentum, and energy yields the Rankine-Hugoniot equations relating u_2 and T_2 to u_1 and T_1. The variation of n with x is determined by solving a Maxwell transport equation for some quantity which is not a summational invariant in the collision integral. Mott-Smith chooses, for convenience, the quantity $\xi_x{}^2$, or alternatively $\xi_x{}^3$, and evaluates the collision integral for rigid sphere molecules and for Sutherland molecules. Whatever the choice of the quantity used in the extra transport equation, the solution for the shock-wave velocity profile can be put in the form

$$\frac{Bx}{l} = \log_e\left(\frac{1 - w}{1 + w}\right) \qquad \text{(B30)}$$

where B is a function of the initial Mach number and the viscosity-temperature dependence, as well as of the choice of transport variable. Mott-Smith feels that the solution obtained is sufficiently independent of the latter choice to be a significant approximation to a solution of the complete Boltzmann equation.

The calculation of t_w from distribution function (B29) has not been performed previously but is a very simple extension of the calculation for the wire in a uniform stream. The steady-state energy-balance equation becomes

$$n_1(x)\,\frac{e^{-s_1{}^2/2}}{\sqrt{T_1}}\left[T_1 a(s_1) - (j + 4)T_w f(s_1)\right] +$$

$$n_2(x)\,\frac{e^{-s_2{}^2/2}}{\sqrt{T_2}}\left[T_2 a(s_2) - (j + 4)T_w f(s_2)\right] = 0 \qquad \text{(B31)}$$

The coefficients a and f are again the same functions as listed in equations (B24). The equation on the preceding page may be solved for T_w, from which the dimensionless, normalized variable t_w may be formed:

$$t_w = \frac{2n_1(x)}{n_1(x) + n_2(x)\sqrt{\frac{T_2}{T_1}}\, e^{\frac{-\left(s_2^2 - s_1^2\right)}{2}} \frac{f(s_2)}{f(s_1)}} - 1 \qquad \text{(B32)}$$

The transformation from the dimensionless abscissa Bx/l to the variable y used in the present paper is performed as follows for the Sutherland molecular model, which is considerably more appropriate to the present purposes than is the rigid sphere model: By Mott-Smith's definition,

$$l = \frac{1}{\sqrt{2}\pi n_1 \sigma^2} \qquad n_1 = n(x) \text{ at } x = -\infty$$

From reference 17, page 184, the viscosity according to the Sutherland model is

$$\mu = \frac{5}{16\sigma^2}\sqrt{\frac{mkT}{\pi}}\,\frac{T}{T + S}$$

Thus, the ratio of the reference length L_* to Mott-Smith's reference length l is

$$\frac{L_*}{l} = \frac{5}{16}\sqrt{2\pi\left(\frac{j+3}{j+5}\right)\left[\left(\frac{j+3}{j+4}\right)\frac{1}{M_1^2} + \frac{1}{j+4}\right]}\,\frac{T_*}{T_* + S} \qquad \text{(B33)}$$

The new symbol S represents the Sutherland constant for the particular gas of interest and is determined by best fit of the experimental viscosity data. Comparison of equations (B30), (B31), and (B18) yields the Mott-Smith shock profile in terms of w and y:

$$y = \left(\frac{j+4}{j+5}\right)\frac{\left(\frac{3\kappa}{4\mu} + 1\right)\mathrm{Pr}}{2 + (j+3)\left(\frac{\kappa}{\mu} + \frac{4}{3}\right)\mathrm{Pr}}\,\frac{\epsilon}{B(M_1)}\,\frac{l}{L_*}\log_e\left(\frac{1-w}{1+w}\right) \qquad \text{(B34)}$$

The function $B(M_1)$ is tabulated for the ξ_x^2 transport and the Sutherland model in reference 13. The introduction of viscosity coefficients and Prandtl number into the shock-profile specification in this case is only an artificial device allowing comparison with shock profiles calculated by other methods, since these macroscopic gas properties do not enter the Mott-Smith method.

This method has been applied here to the calculation of shocks in helium at $M_1 = 1.61$ ($\epsilon = 1.5$) and $M_1 = 1.82$ ($\epsilon = 1.77$) and in air at $M_1 = 1.89$ ($\epsilon = 3$) and $M_1 = 3.70$ ($\epsilon = 4.40$), the results being shown in figures 15(a) to 15(c) and 16.

APPENDIX C

EQUILIBRIUM TEMPERATURE OF A FREE-MOLECULE CYLINDER IN A DIATOMIC GAS WITH ROTATIONAL RELAXATION

Since the equilibrium temperature of a free-molecule cylinder is considerably higher in a monatomic gas stream than in a diatomic gas with the same velocity and temperature, the following calculation has been carried out to predict the temperature of the cylinder in a diatomic gas whose inert degrees of freedom are out of equilibrium with the translational degrees of freedom. An application of the analysis is made to the hypothetical case of a cylinder placed just downstream of the first zone of a normal shock wave followed by a rotational relaxation zone of comparatively infinite length. This is the shock whose properties have been analyzed in references 20, 21, and 22.

The distribution function for the relaxing diatomic molecules is taken to be Maxwellian in form, and it is assumed that it may be factored into a translational term and a rotational term as follows:

$$f = n\left(\frac{m}{2\pi kT}\right)^{3/2} \frac{1}{\sum_s e^{-E_{Rs}/kT_R}} e^{-mC^2/2kT_t} e^{-E_R/kT_R} \qquad (C1)$$

where E_{Rs} is the rotational energy of a molecule in the sth rotational state. This is the standard approach to the free-molecule analysis of uniform polyatomic gas flows (ref. 28), the only difference being that it is now proposed to assign different values to the translational temperature T_t and to the rotational temperature T_R. In addition, separate accommodation coefficients for translational and rotational energies α_t and α_R are introduced, defined by:

$$\alpha_t = \frac{dE_{ti} - dE_{tr}}{dE_{ti} - dE_{tw}}$$

$$\alpha_R = \frac{dE_{Ri} - dE_{Rr}}{dE_{Ri} - dE_{Rw}}$$

In each of these defining equations dE represents an average energy flux crossing an infinitesimal section of the interface between gas and solid, the first subscript indicates the type of molecular energy (translational or rotational), and the second subscript has the following meanings:

i	pertaining to incident molecules
r	pertaining to reemitted molecules
w	pertaining to hypothetical molecules being reemitted in Maxwellian equilibrium at temperature of solid wall

Since the T's and α's are taken as constants in the problem of determining the equilibrium temperature of a cylinder, these modified concepts have no effect on the integrations over the energy spaces and around the circumference of the wire. The desired results may be drawn from the calculations of reference 28 and will be expressed here in the nomenclature of appendix B:

$$2\frac{T_w}{T_t} = \frac{\alpha_t}{2\alpha_t + \alpha_R}\frac{a(s)}{f(s)} + \frac{2\alpha_R}{2\alpha_t + \alpha_R}\frac{T_R}{T_t} \tag{C2}$$

In this equation the molecular speed ratio is based on the translational temperature alone; that is,

$$s = \frac{u}{\sqrt{2kT_t}} \tag{C3}$$

The speed-ratio functions $a(s)$ and $f(s)$ are those given in equations (B24), with $j = 0$.

Various special cases obtain from different assumptions concerning the relative magnitude of α_t and α_R. For instance, one might argue that, if the gas molecules require an enormous number of collisions among themselves in order to restore equipartition of energy between translation and rotation, the rotational energy may be negligibly accommodated to the temperature of an immersed solid surface, so that approximately $\alpha_R/\alpha_t = 0$. Then the energy balance would reduce to

$$\frac{T_w}{T_t} = \frac{1}{4}\frac{a(s)}{f(s)} \tag{C4}$$

which is simply the result for a monatomic gas.

If, on the other hand, one subscribes to the notion of a gas molecule being momentarily absorbed by a solid surface and then reevaporated with little or no memory of its past history, it may appear that a collision with the cylinder is sufficiently more serious than a simple collision between gas molecules so that the reluctant rotational energy may be accommodated as well as the translational energy.[4] Setting $\alpha_R = \alpha_t$ brings about the special energy-balance equation

$$\frac{T_w}{T_t} = \frac{1}{6}\frac{a(s)}{f(s)} + \frac{1}{3}\frac{T_R}{T_t} \tag{C5}$$

Without attempting at once to decide which of these hypotheses seems the more reasonable, both may be applied to the prediction of the cylinder equilibrium temperature in a flow where T_t is the translational temperature immediately downstream of a shock which was too sudden for T_R to have made any appreciable adjustment away from its upstream equilibrium value. The result will be compared with the temperature which the cylinder would have behind a shock initiating with the same upstream conditions but displaying no rotational heat lag.

The ratio T_R/T_t and s for the station immediately behind the first shock front must be computed. Since T_R, the equilibrium-state temperature upstream of the shock, is already known, the unknowns are T_t and u. They may be calculated algebraically by considering one-dimensional flow through a plane in which the specific-heats ratio of the gas changes from 7/5 to 5/3, with mass, momentum, and energy being conserved. A convenient technique employing published gas-dynamics tables is as follows:

(1) Corresponding to the initial Mach number M_1, calculate a "monatomic" Mach number M_{1m} by

$$M_{1m} = \sqrt{\frac{7/5}{5/3}}\,M_1 = 0.9165M_1 \tag{C6}$$

---

[4]Knudsen (ref. 41) reached this conclusion for hydrogen and platinum.

(2) Look up T_{t2}/T_{t1} and M_{2m} opposite M_{1m} in tables of normal-shock functions for a monatomic gas. Then the quantities needed for the problem are obtained simply from

$$\left(\frac{T_R}{T_t}\right)_2 = \frac{T_{t1}}{T_{t2}} \tag{C7}$$

since $T_{R2} = T_{R1} = T_{t1}$ and

$$s_2 = \sqrt{\frac{5}{6}}\, M_{2m} \tag{C8}$$

(3) Calculate T_w/T_{t2} from equation (C4) or from equation (C5).

(4) Suppose that the upstream flow has a stagnation temperature T_o so that T_{t1}/T_o can be found opposite M_1 in adiabatic-flow tables of a diatomic gas. Then T_w may be referred to T_o by the equation

$$\frac{T_w}{T_o} = \frac{T_w}{T_{t2}} \frac{T_{t2}}{T_{t1}} \frac{T_{t1}}{T_o}$$

For comparison, T_w/T_o for the case with no rotational lag may be read from figure 11 opposite the Mach number M_2, which is given as a function of M_1 in diatomic-gas normal-shock tables.

In this manner the ratio T_w/T_o versus M_1 has been computed and graphed in figure 17 for the three cases (a) with no relaxation zone behind the shock, (b) with an extended relaxation zone and with zero accommodation of rotational molecular energy to the surface temperature of the wire, and (c) with relaxation and with equal accommodation of rotational and translational energies.

REFERENCES

1. Rankine, W. J. Macquorn: On the Thermodynamic Theory of Waves of Finite Longitudinal Disturbance. Phil. Trans. Roy. Soc. (London), vol. 160, pt. 2, 1870, pp. 277-288.

2. Rayleigh, Lord: Aerial Plane Waves of Finite Amplitude. Proc. Roy. Soc. (London), ser. A, vol. 84, no. 570, July 8, 1910, pp. 247-284.

3. Taylor, G. I.: The Conditions Necessary for Discontinuous Motion in Gases. Proc. Roy. Soc. (London), ser. A, vol. 84, no. 571, July 11, 1910, pp. 371-377.

4. Becker, R.: Stosswelle und Detonation. Zs. Phys., Bd. 8, 1922, pp. 321-362. (Available in English translation as NACA TM 505 and TM 506.)

5. Thomas, L. H.: Note on Becker's Theory of the Shock Front. Jour. Chem. Phys., vol. 12, no. 11, Nov. 1944, pp. 449-453.

6. Tani, Itiro: Numerical Calculation of the Transition Layer of a Shock Wave. Rep. No. 246, Aero. Res. Inst., Tokyo Imperial Univ., Feb. 1945, pp. 63-65.

7. Wang Chang, C. S.: On the Theory of the Thickness of Weak Shock Waves. Rep. UMH-3-F, Dept. Eng. Res., Univ. of Mich., Aug. 1948; also CM-503, Appl. Phys. Lab., The Johns Hopkins Univ.

8. Morduchow, Morris, and Libby, Paul A.: On a Complete Solution of the One-Dimensional Flow Equations of a Viscous, Heat-Conducting, Compressible Gas. Jour. Aero. Sci., vol. 16, no. 11, Nov. 1949, pp. 674-684, 704.

9. Puckett, A. E., and Stewart, H. J.: The Thickness of a Shock Wave in Air. Quart. Appl. Math., vol. VII, no. 4, Jan. 1950, pp. 457-463.

10. Von Mises, R.: On the Thickness of a Steady Shock Wave. Jour. Aero. Sci., vol. 17, no. 9, Sept. 1950, pp. 551-554, 594.

11. Meyerhoff, Leonard: An Extension of the Theory of the One-Dimensional Shock-Wave Structure. Jour. Aero. Sci., vol. 17, no. 12, Dec. 1950, pp. 775-786.

12. Zoller, K.: Zur Struktur des Verdichtungsstosses. Zs. Phys., Bd. 130, Heft 1, 1951, pp. 1-38.

13. Mott-Smith, H. M.: The Solution of the Boltzmann Equation for a Shock Wave. Phys. Rev., ser. 2, vol. 82, no. 6, June 15, 1951, pp. 885-892.

14. Shapiro, A. H., and Kline, S. J.: On the Thickness of Normal Shock Waves in a Perfect Gas. Jour. Appl. Mech., vol. 21, June 1954, pp. 185-192.

15. Grad, H.: The Profile of a Steady Plane Shock Wave. Com. Pure and Appl. Math., vol. V, no. 3, Aug. 1952, pp. 257-300.

16. Gilbarg, D., and Paolucci, D.: The Structure of Shock Waves in the Continuum Theory of Fluids. Jour. Rational Mech. and Analysis, vol. 2, no. 4, 1953, pp. 617-642.

17. Chapman, Sydney, and Cowling, T. G.: The Mathematical Theory of Non-Uniform Gases. Univ. Press (Cambridge), 1939.

18. Grad, H.: On the Kinetic Theory of Rarefied Gases. Com. Pure and Appl. Math., vol. II, no. 4, Dec. 1949, pp. 331-407.

19. Truesdell, C.: Precise Theory of the Absorption and Dispersion of Forced Plane Infinitesimal Waves According to the Navier-Stokes Equations. Jour. Rational Mech. and Analysis, vol. 2, no. 4, 1953, pp. 643-741.

20. Stepanoff, P. E.: On the Relaxation Phenomena in a Shock Wave in Gas. Jour. Exp. and Theor. Phys. (USSR), vol. 17, no. 5, 1947, pp. 377-385. (In Russian.)

21. Broer, L. J. F.: On the Influence of Acoustic Relaxation on Compressible Flow. Appl. Sci. Res., vol. A2, nos. 5 and 6, 1951, pp. 447-468.

22. Gould, D. G.: The Head-On Collision of Two Shock Waves and a Shock and Rarefaction Wave in One-Dimensional Flow. Rep. No. 17, Inst. Aerophys., Univ. of Toronto, May 1952.

23. Cowan, George R., and Hornig, D. F.: The Thickness of a Shock Front in a Gas. Tech. Rep. No. 1, Contract N7onr-358, Task Order 3, Office of Naval Res. and Metcalf Res. Lab., Brown Univ., Apr. 6, 1949.

24. Greene, E. F., Cowan, G. R., and Hornig, D. F.: The Thickness of Shock Fronts in Argon and Nitrogen and Rotational Heat Capacity Lags. Jour. Chem. Phys., vol. 19, no. 4, Apr. 1951, pp. 427-434.

25. Greene, E. F., and Hornig, D. F.: The Shape and Thickness of Shock Fronts in Argon, Hydrogen, Nitrogen, and Oxygen. Tech. Rep. No. 4, Contract N7-onr-358, Task Order 3, Office of Naval Res. and Metcalf Res. Lab., Brown Univ., Aug. 1, 1952.

26. Tsien, Hsue-Shen: Wind-Tunnel Testing Problems in Superaerodynamics. Jour. Aero. Sci., vol. 15, no. 10, Oct. 1948, pp. 573-580.

27. Stalder, Jackson R., and Jukoff, David: Heat Transfer to Bodies Traveling at High Speed in the Upper Atmosphere. NACA Rep. 944, 1949. (Supersedes NACA TN 1682.)

28. Stalder, Jackson R., Goodwin, Glen, and Creager, Marcus O.: A Comparison of Theory and Experiment for High-Speed Free-Molecule Flow. NACA Rep. 1032, 1951. (Supersedes NACA TN 2244.)

29. Stalder, Jackson R., Goodwin, Glen, and Creager, Marcus O.: Heat Transfer to Bodies in a High-Speed Rarefied-Gas Stream. NACA Rep. 1093, 1952. (Supersedes NACA TN 2438.)

30. Bell, S.: Heat Transfer to a Cylinder for the Free-Molecule Flow of a Non-Uniform Gas. Rep. HE-150-115, Contract N7-onr-295, Office of Naval Res., Office of Sci. Res., and Inst. Eng. Res., Univ. of Calif., Sept. 14, 1953.

31. Kunkel, W. B.: Mass Production and Some Properties of Intense RF Excited Afterglows in Air and Nitrogen. Rep. HE-150-106, Contract AF-33(038)8896, WADC and Eng. Res. Projects, Univ. of Calif., Aug. 1952.

32. Schaaf, S. A., Horning, Don O., and Kane, E. D.: Design and Initial Operation of a Low Density Supersonic Wind Tunnel. Rep. HE-150-62, Contract No. N7-ONR-295-Task 3, Office of Naval Res. and Eng. Res. Projects, Univ. of Calif., Aug. 15, 1949.

33. Owen, J. M., and Sherman, F. S.: Design and Testing of a Mach 4 Axially Symmetric Nozzle for Rarefied Gas Flows. Rep. HE-150-104, Contract No. N7-onr-295, Office of Naval Res., Office of Sci. Res., and Inst. Eng. Res., Univ. of Calif., July 23, 1952.

34. Nuttall, R. L.: Helium - Coefficient of Viscosity η/η_0. NBS-NACA Tables of Thermal Properties of Gases, Table 6.39, Dec. 1950.

35. Morey, F. C.: Dry Air - Coefficients of Viscosity η/η_0, ν/ν_0. NBS-NACA Tables of Thermal Properties of Gases, Table 2.39, Dec. 1950.

36. Truesdell, C.: The Mechanical Foundations of Elasticity and Fluid Dynamics. Jour. Rational Mech. and Analysis, vol. 1, no. 1, 1952, pp. 125-171; no. 2, 1952, pp. 172-300; also, Corrections and Additions to "The Mechanical Foundations of Elasticity and Fluid Dynamics." Jour. Rational Mech. and Analysis, vol. 2, no. 3, 1953, pp. 593-616.

37. Wang Chang, C. S., and Uhlenbeck, G. E.: Transport Phenomena in Polyatomic Gases. Rep. No. CM-681, Eng. Res. Inst., Univ. of Mich., July 1951.

38. Scadron, Marvin D., and Warshawsky, Isidore: Experimental Determination of Time Constants and Nusselt Numbers for Bare-Wire Thermocouples in High-Velocity Air Streams and Analytic Approximation of Conduction and Radiation Errors. NACA TN 2599, 1952.

39. Gier, J. T., and Dunkle, R. V.: Quart. Prog. Rep. No. 1, Thermal Radiation Project, Contract N7-onr-295, Task 1, Office of Naval Res. and Eng. Res. Projects, Univ. of Calif., Apr. 1 - Aug. 1, 1947.

40. Oliver, Robert N., and Farber, Milton: Experimental Determination of Accommodation Coefficients as Functions of Temperature for Several Metals and Gases. Memo. 9-19, Contract DA-04-495-ORD-18, Ordnance Dept. and Jet Propulsion Lab., C.I.T., Nov. 20, 1950.

41. Knudsen, M.: Radiometerdruck und Akkommodationskoeffizient. Ann. Phys., Folge 5, Bd. 6, Heft 2, Aug. 16, 1930, pp. 129-185.

TABLE I

SUMMARY OF FLOW PROPERTIES

[Assumed stagnation temperature, 530° R]

Nozzle	Gas	Flow rate, lb/hr	M_1	ϵ	ρu, lb-sec/ft^3	Λ_1, ft (a)	L_*, ft (b)	y/x, ft^{-1} (c)
6	Helium	2.88	1.72	1.65	0.000312	0.00232	0.00108	174
6	Helium	3.84	1.82	1.77	.000390	.00189	.000864	233
6	Air	2.6	1.78	2.79	.000268	.00254	.00184	154
6	Air	3.9	1.85	2.94	.000380	.00182	.00130	230
6	Air	5.2	1.90	3.02	.000483	.00146	.00102	301
6	Air	7.7	1.98	3.15	.000670	.00106	.000736	434
8	Air	5.2	3.70	4.40	.001280	.000513	.000386	1,157
8	Air	10.3	3.91	4.46	.002058	.000305	.000240	1.886

[a]Mean free path ahead of shock, $\Lambda_1 = \sqrt{\frac{\pi}{2}\left(\frac{j+5}{j+3}\right)}\frac{M_1\mu_1}{\rho u}$.

[b]For helium, $L_* = \mu_*/\rho u$; for air, $L_* = \frac{3}{2}\frac{\mu_*}{\rho u}$.

[c]For helium, $y = \frac{4}{35}\frac{\epsilon x}{L_*}$; for air (Bulk viscosity = Two-thirds shear viscosity), $y = \frac{27}{266}\frac{\epsilon x}{L_*}$.

TABLE II

THEORETICAL SHOCK PROFILES ACCORDING TO NAVIER-STOKES EQUATIONS

Gas	M_1	ϵ	j	Pr	κ/μ	λ^{int}/λ	$\omega\left(\text{in } \mu \propto T^{\omega}\right)$
[a]Helium	1.61	1.5	0	2/3	0	0	0.663
[a]Helium	1.82	1.78	0	2/3	0	0	.663
Air	1.89	3	2	3/4	0	2/5	.76
[a]Air	1.89	3	2	3/4	2/3	2/5	.76
Air	3.70	4.4	2	3/4	0	2/5	.76
Air	3.70	4.4	2	3/4	4/9	2/5	.76
[a]Air	3.70	4.4	2	3/4	2/3	2/5	.76
Air	3.70	4.4	2	[b]Pr(T)	0	2/5	[b]μ(T)

[a]Also treated by Mott-Smith theory, ξ_x^2 transport, and Sutherland molecules.

[b]Empirical variation with temperature (refs. 34 and 35), $T_* = 441.6^{\circ}$ R.

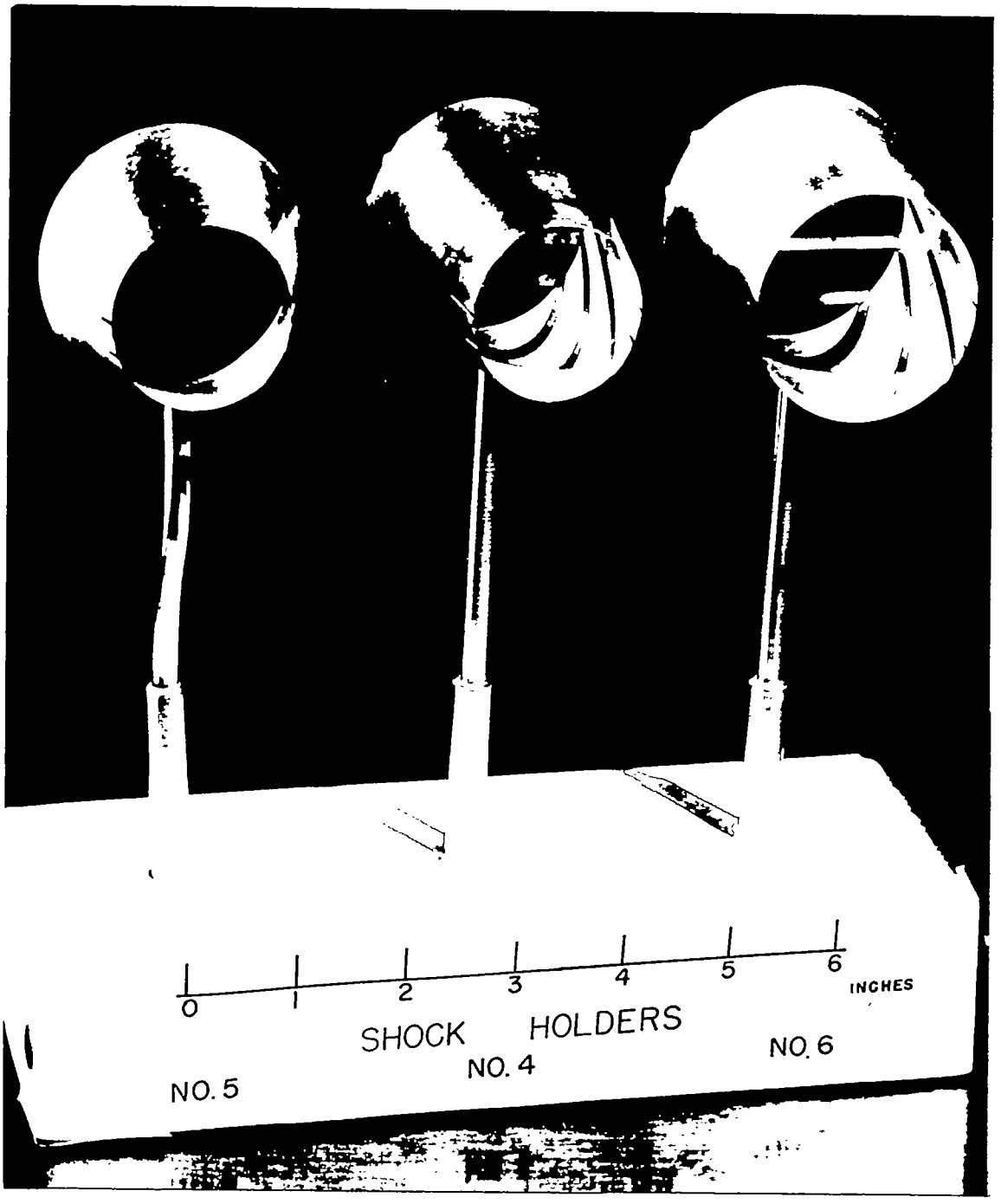

L-87939

Figure 1.- Shock holders.

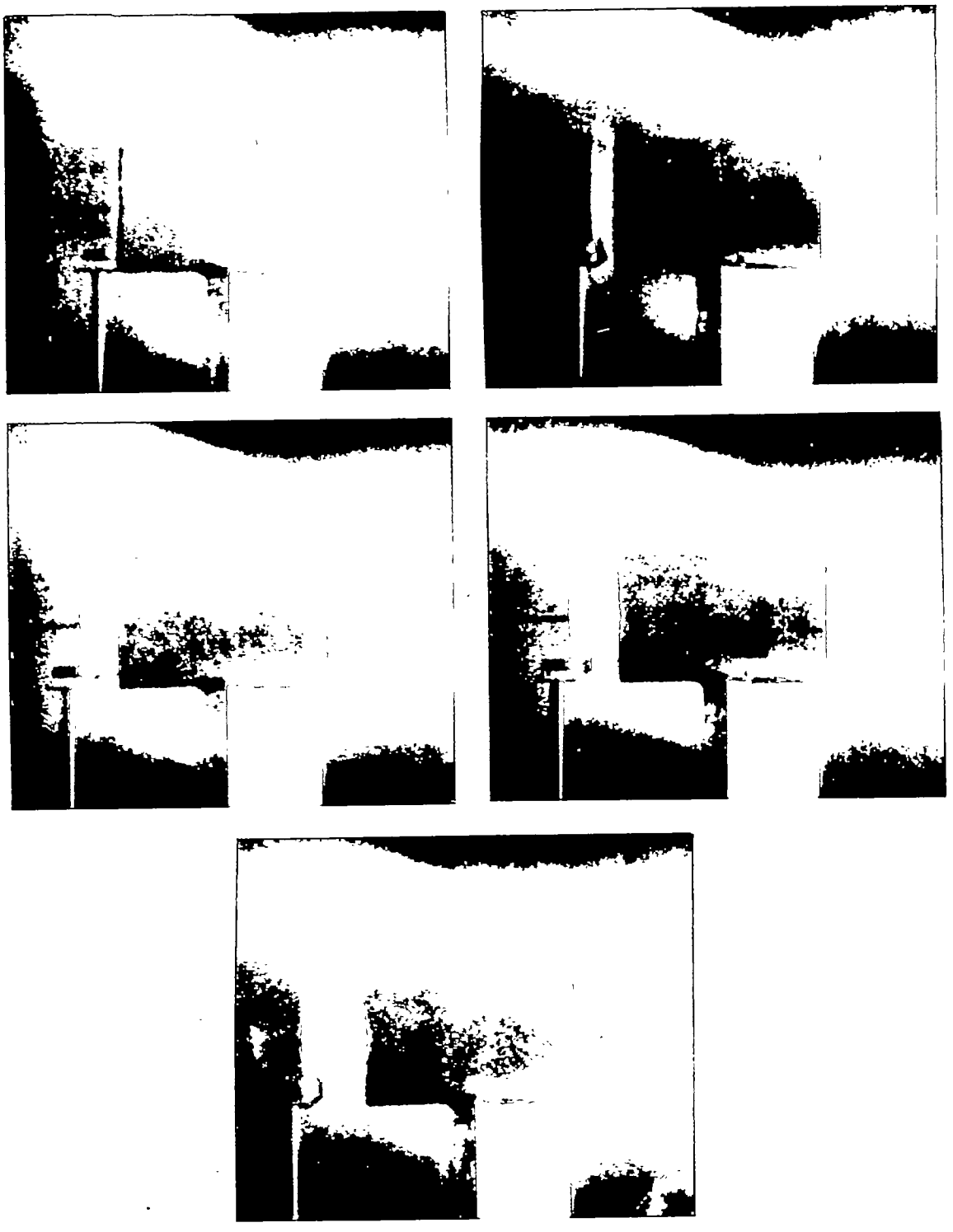

L-87940

Figure 2.- Air-afterglow photos showing principle of shock-holder operation.

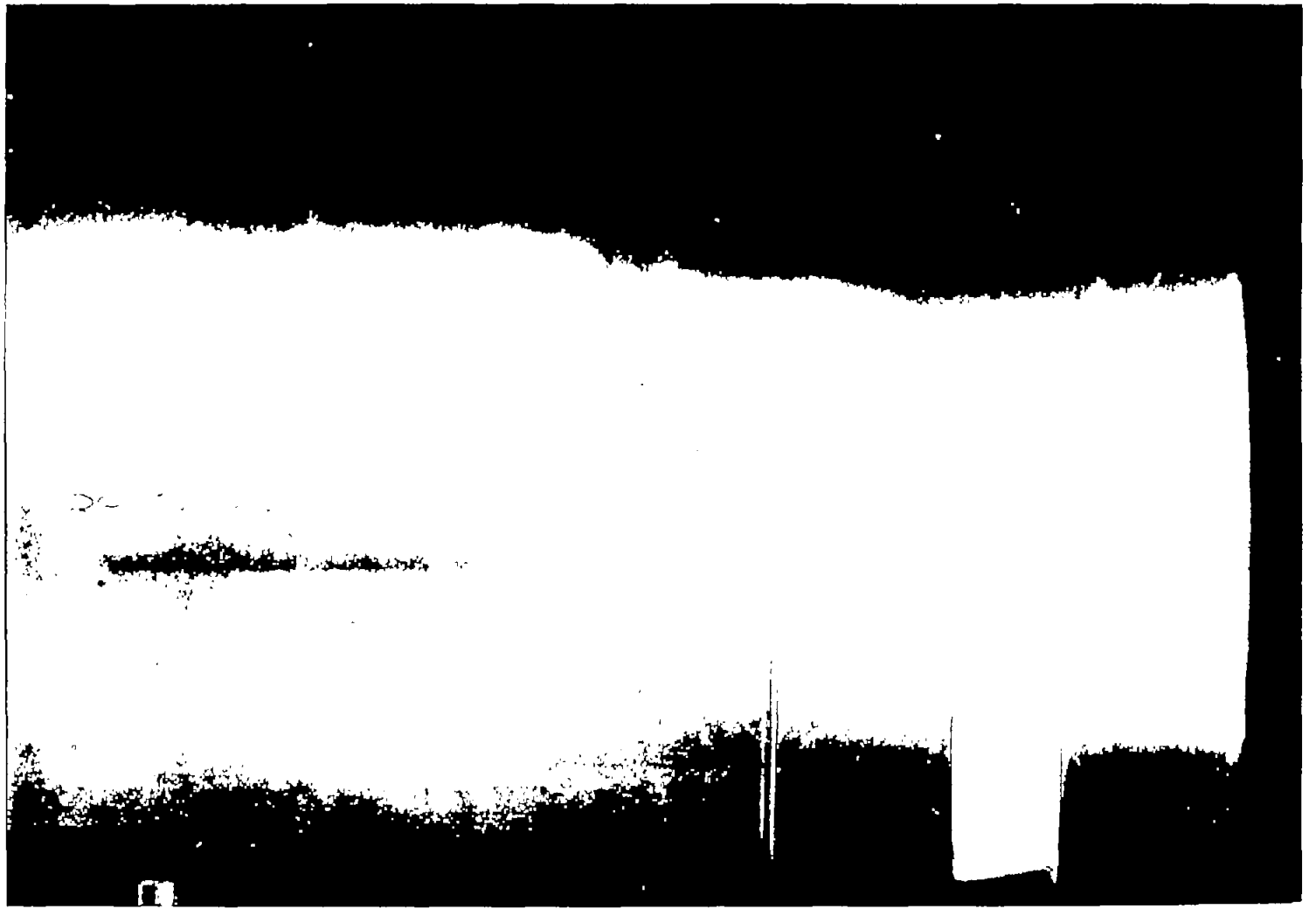

L-87941

Figure 3.- Disturbance of shock by small impact tube.

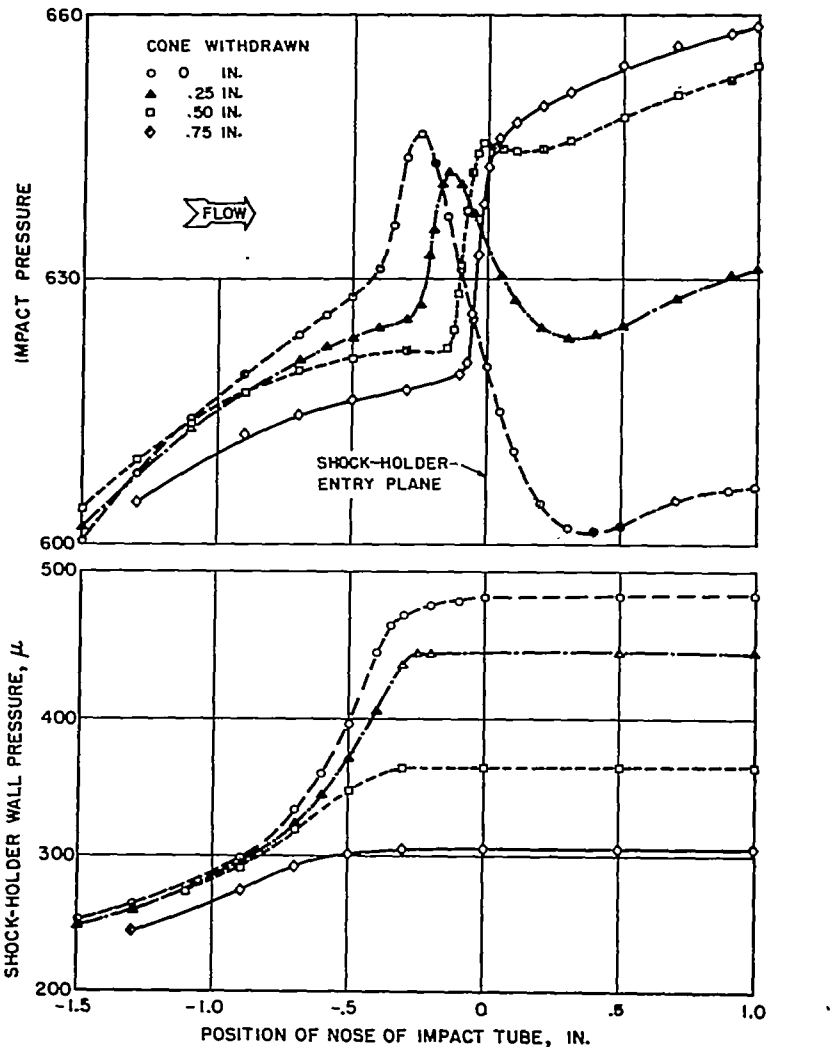

Figure 4.- Shock-wave traces taken with a small impact tube, showing effect of variable choking of shock holder.

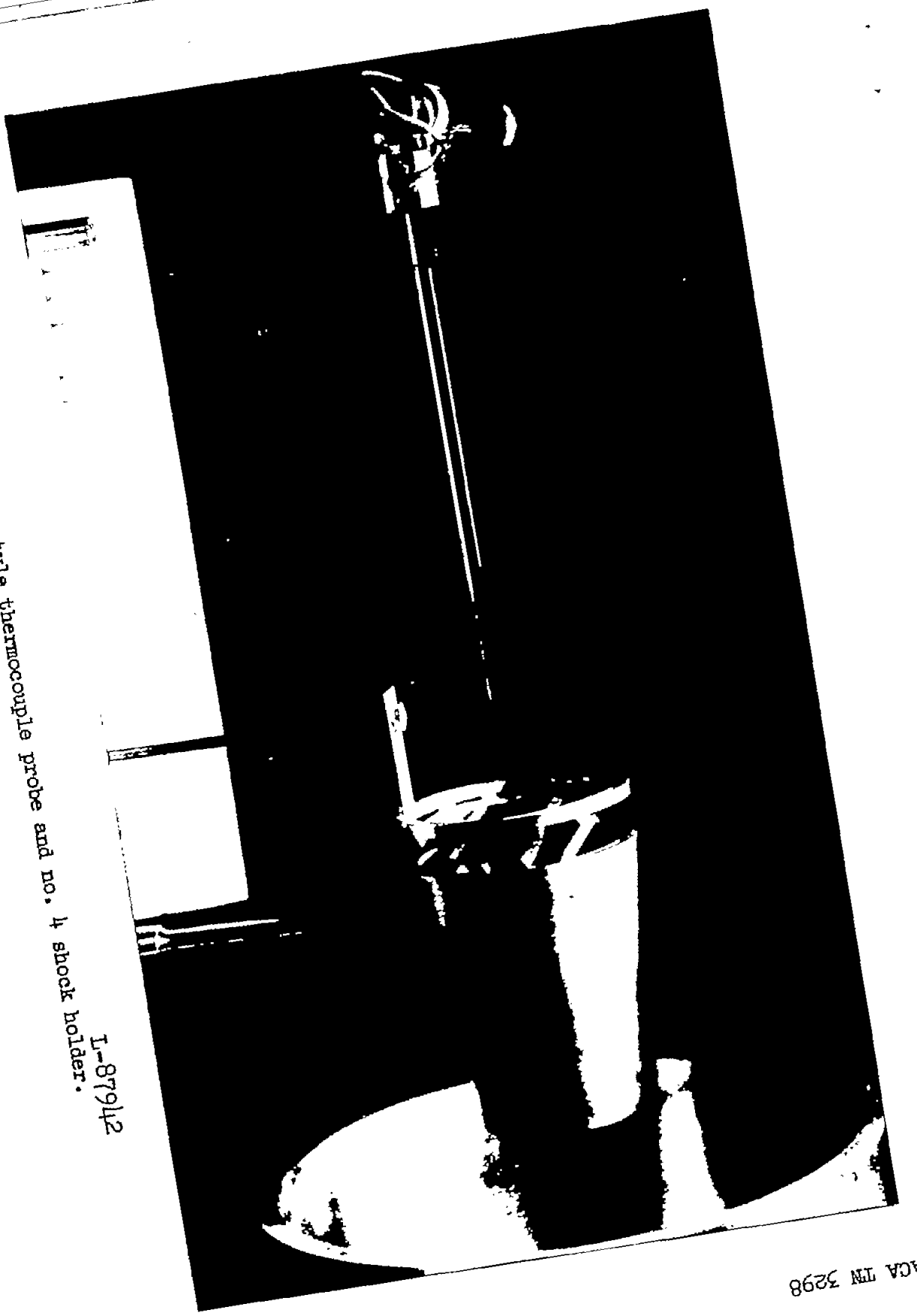

Figure 5.- Early style thermocouple probe and no. 4 shock holder.

L-87942

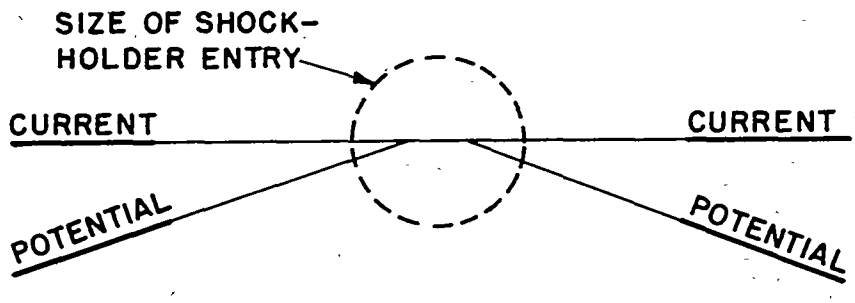

(a) Resistance-wire thermometer.

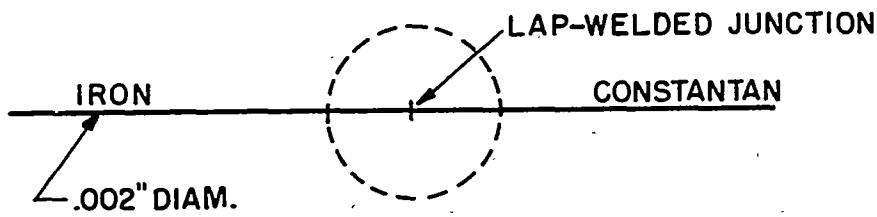

(b) Thermocouple.

Figure 6.- Equilibrium-temperature probes.

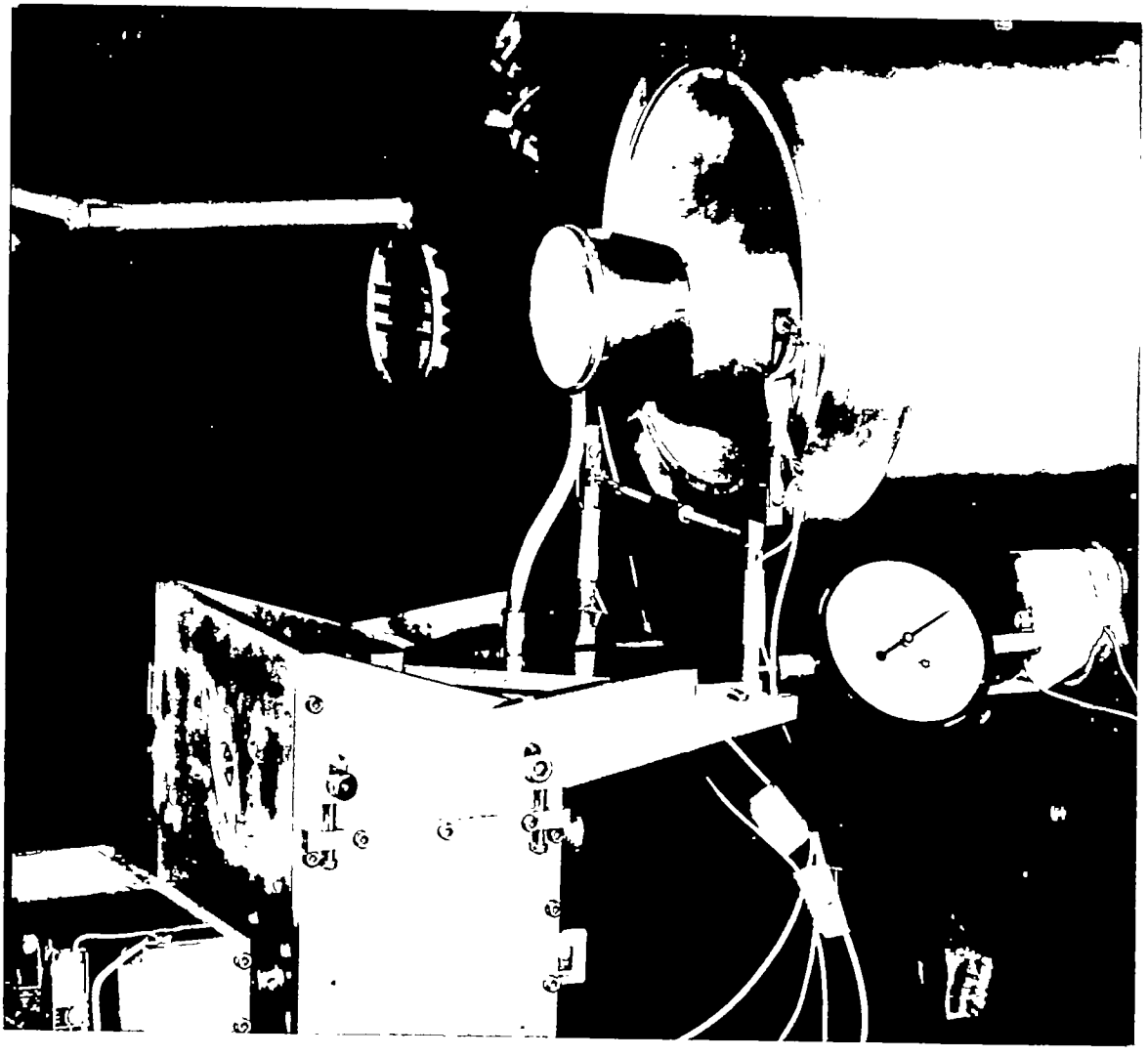

L-87943

Figure 7.- Experimental setup showing nozzle 6, wire traverse, no. 5 shock holder, dial gage, and wiring for resistance thermometer.

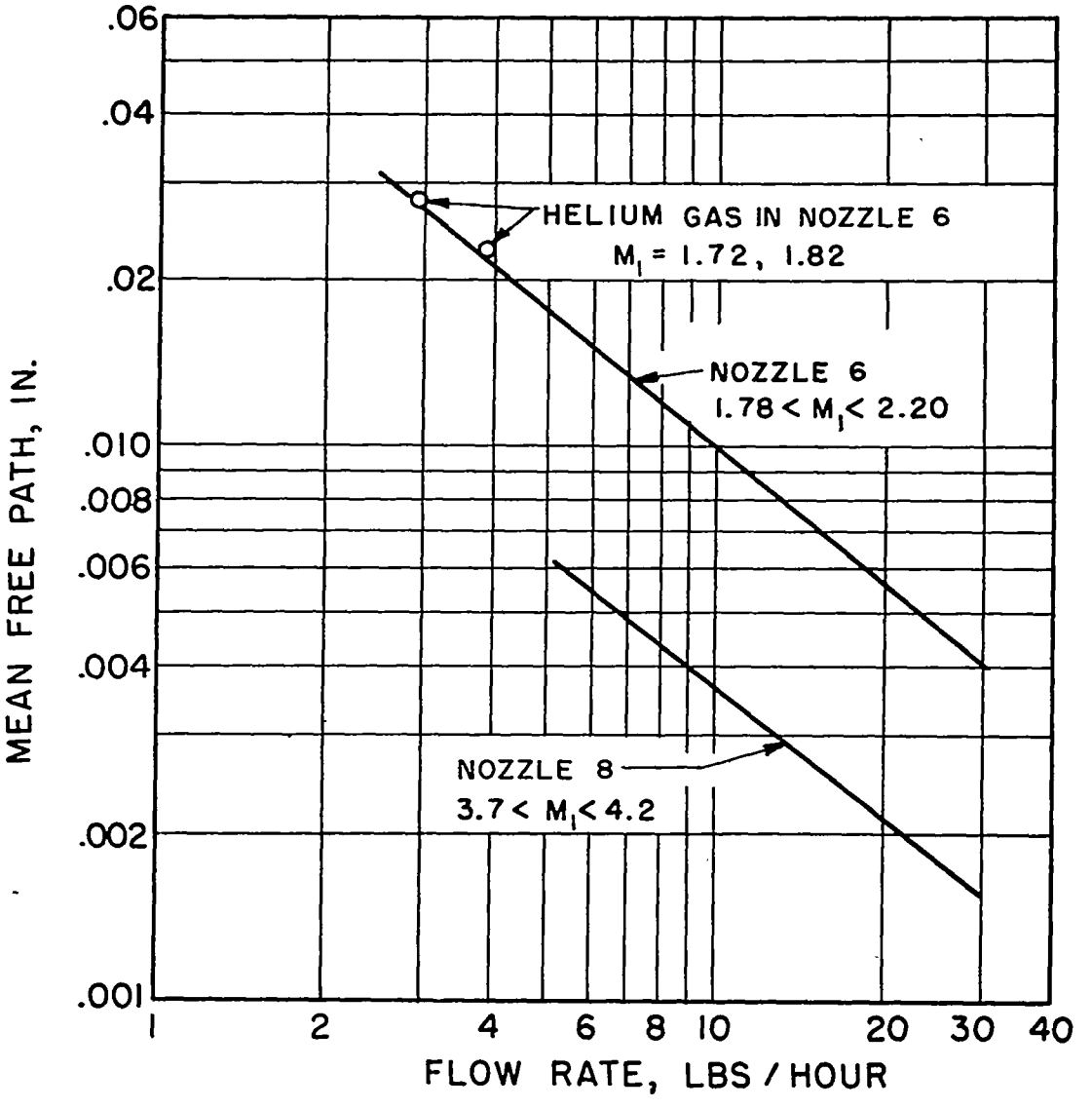

Figure 8.- Mean free path in free stream of no. 3 wind tunnel.

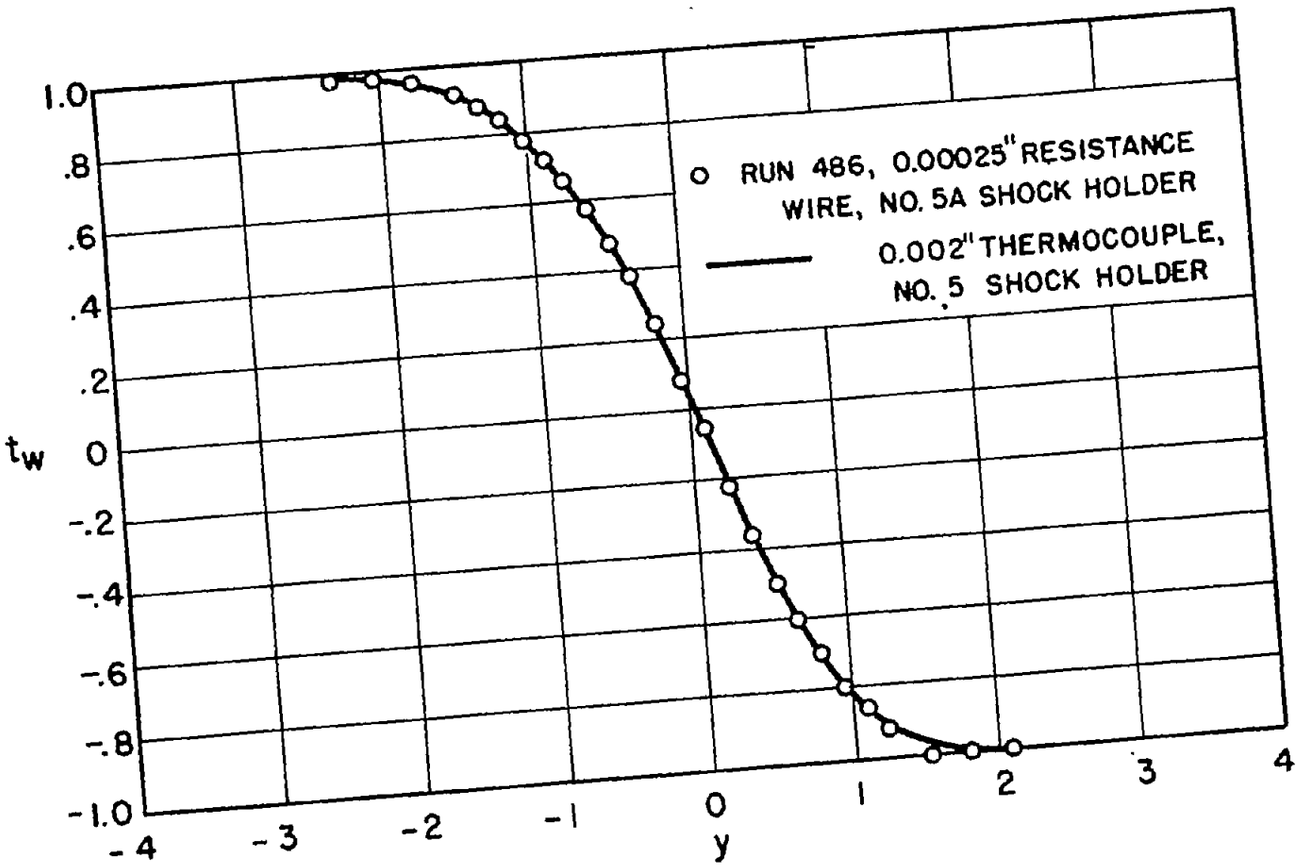

(a) Nozzle 6; 2.9 lb/hr; helium; $M_1 = 1.72$.

Figure 9.- Experimental shock profiles.

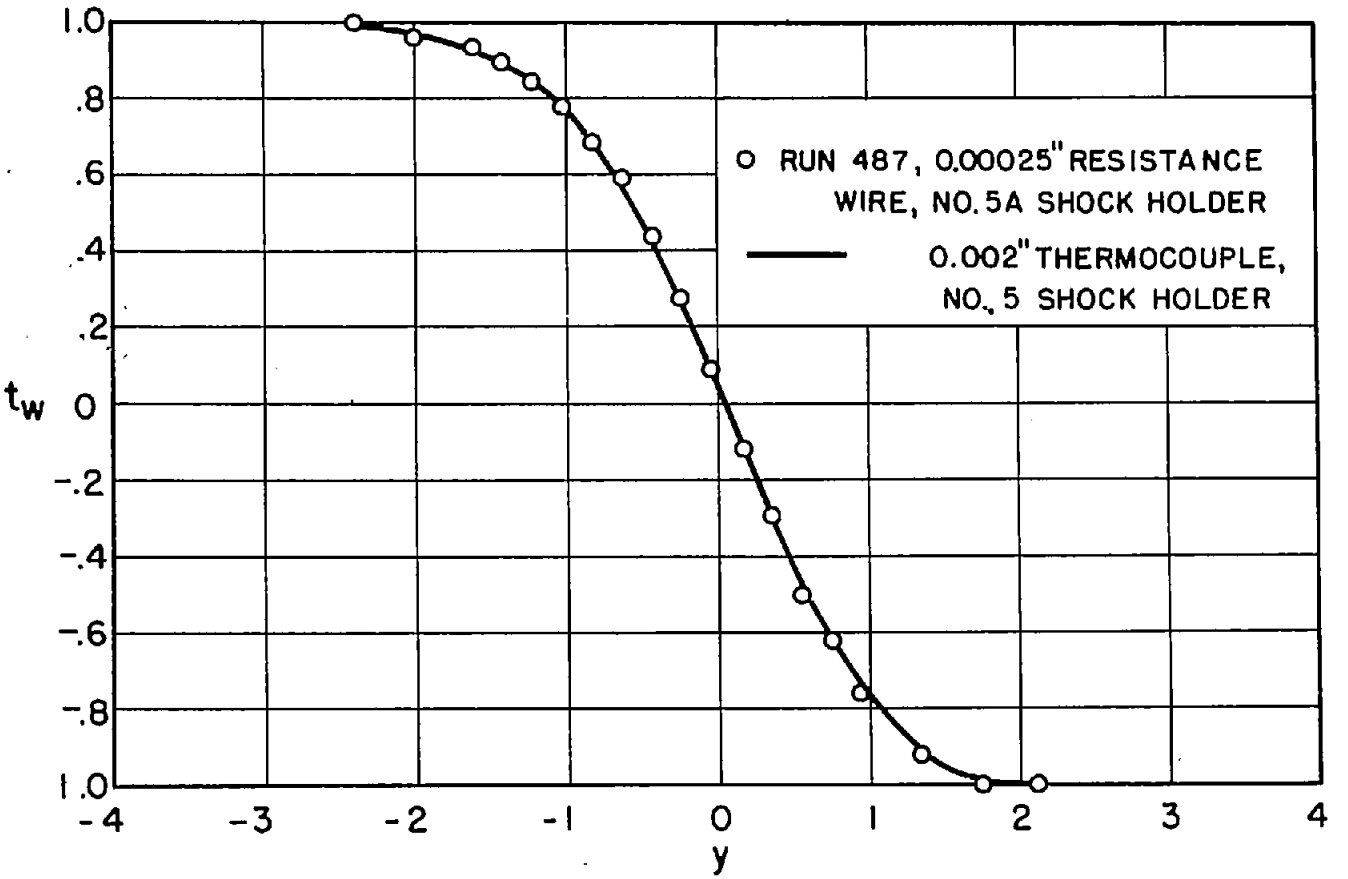

(b) Nozzle 6; 3.8 lb/hr; helium; $M_1 = 1.82$.

Figure 9.- Continued.

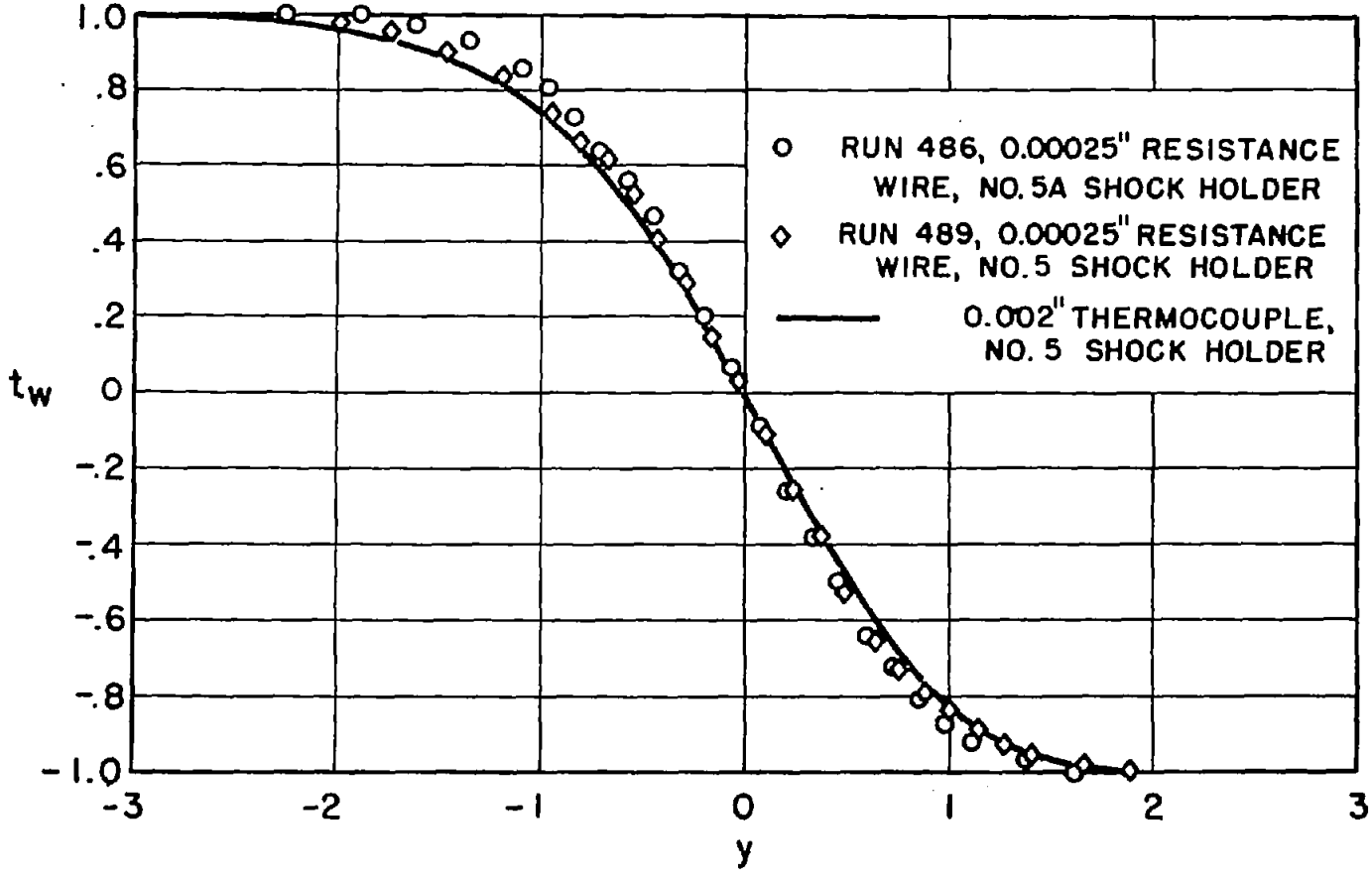

(c) Nozzle 6; 2.6 lb/hr; air; $M_1 = 1.78$.

Figure 9.- Continued.

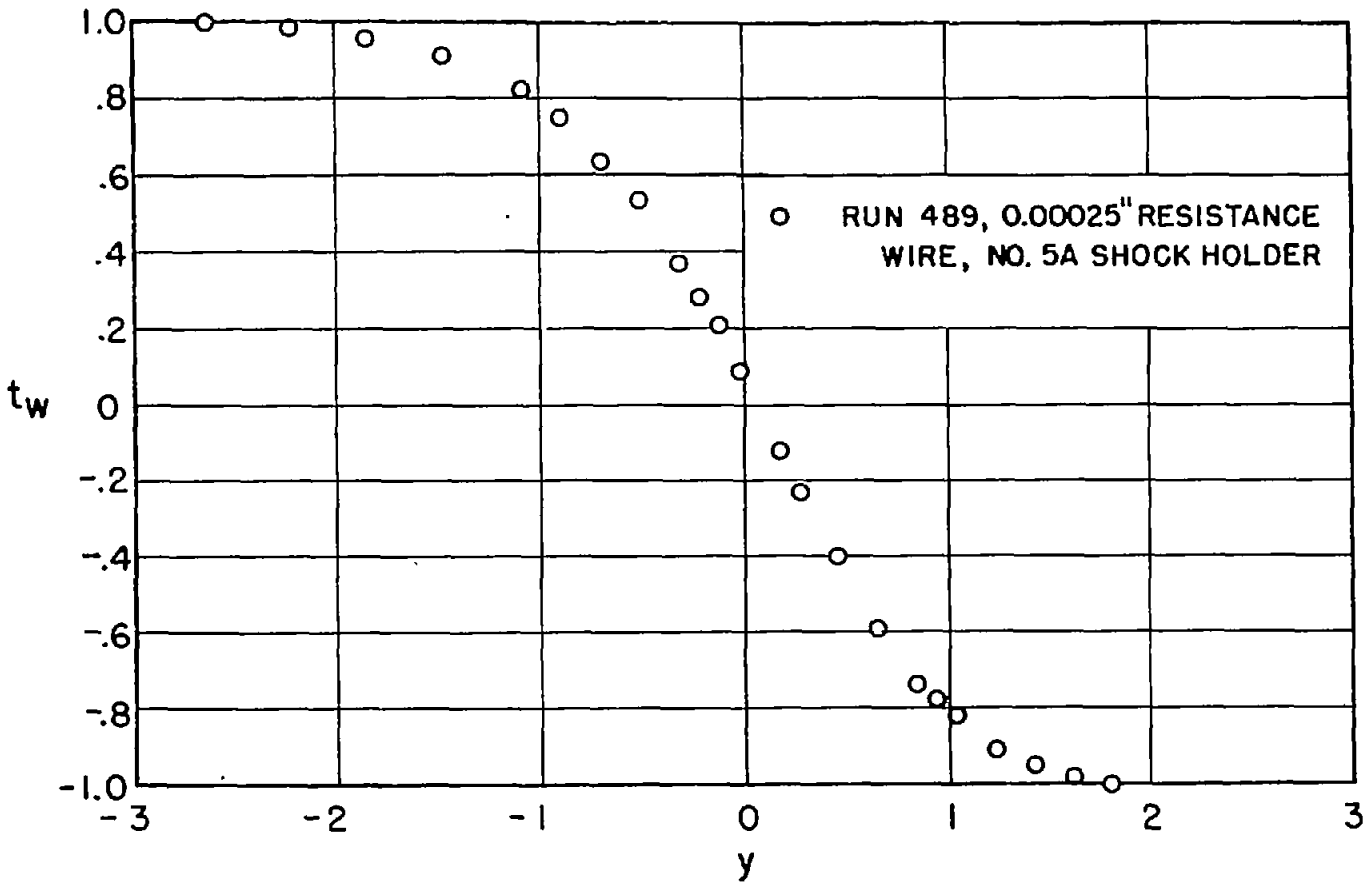

(d) Nozzle 6; 3.9 lb/hr; air; $M_1 = 1.85$.

Figure 9.- Continued.

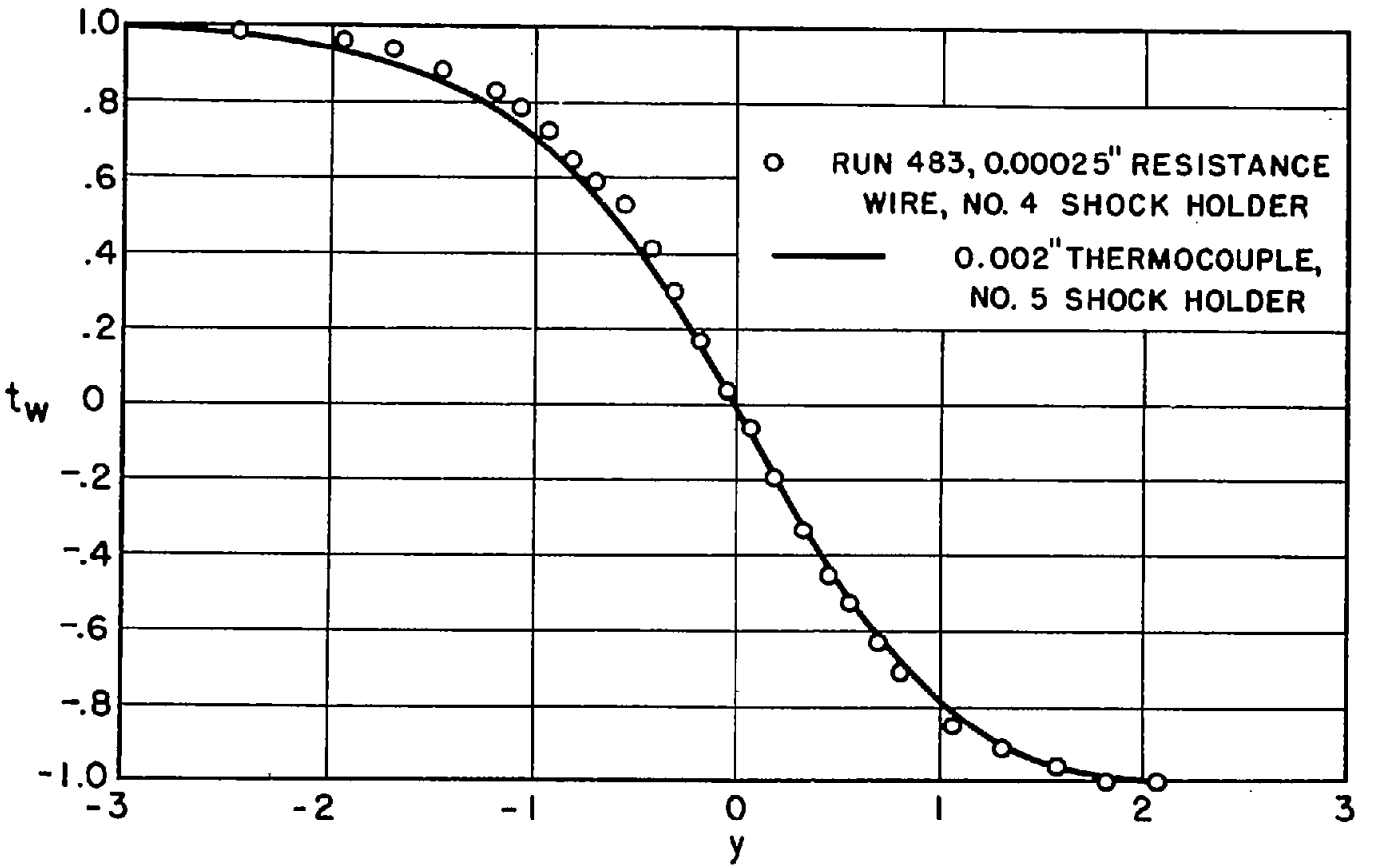

(e) Nozzle 6; 5.2 lb/hr; air; $M_1 = 1.90$.

Figure 9.- Continued.

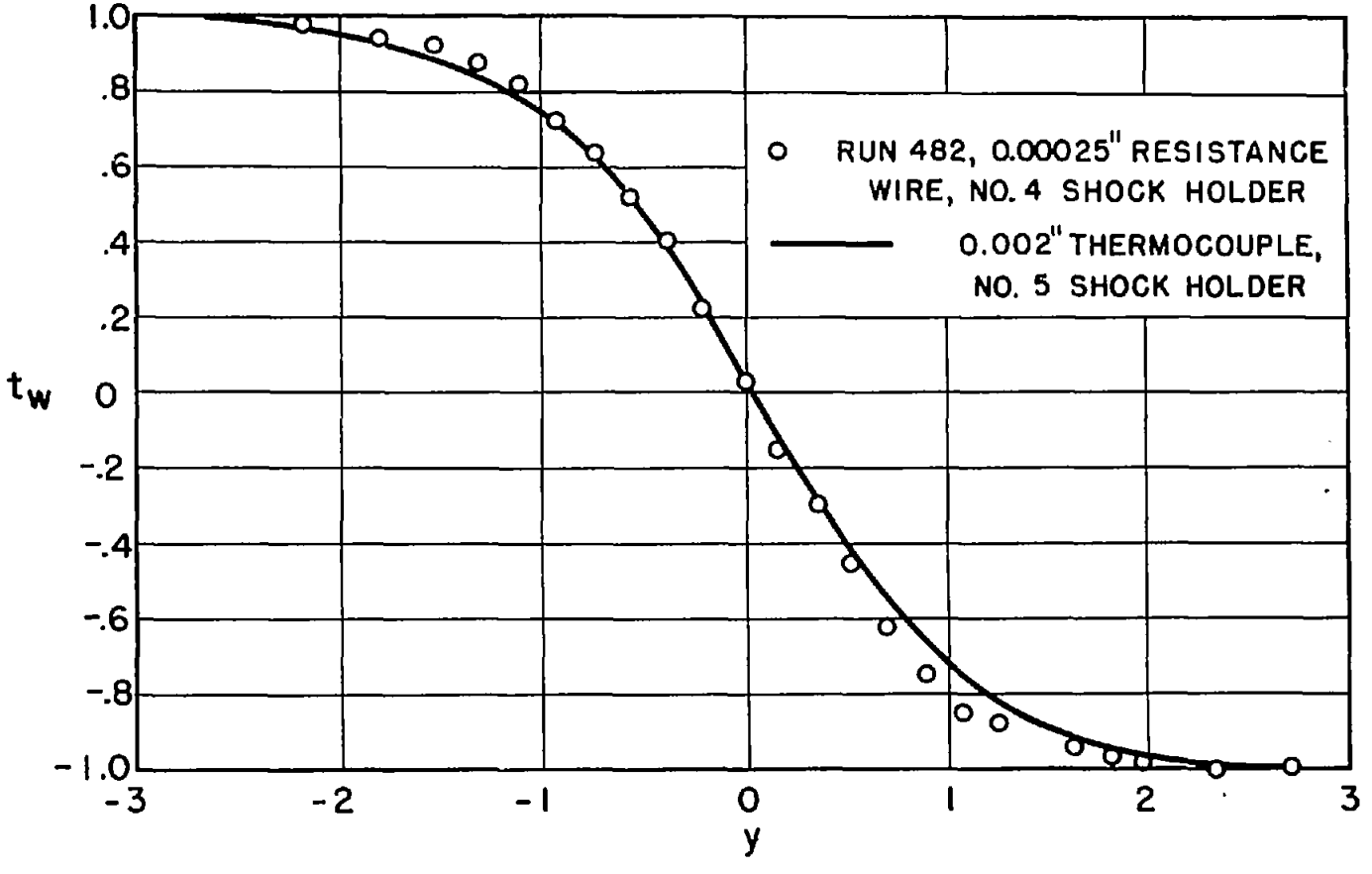

(f) Nozzle 6; 7.7 lb/hr; air; $M_1 = 1.98$.

Figure 9.- Continued.

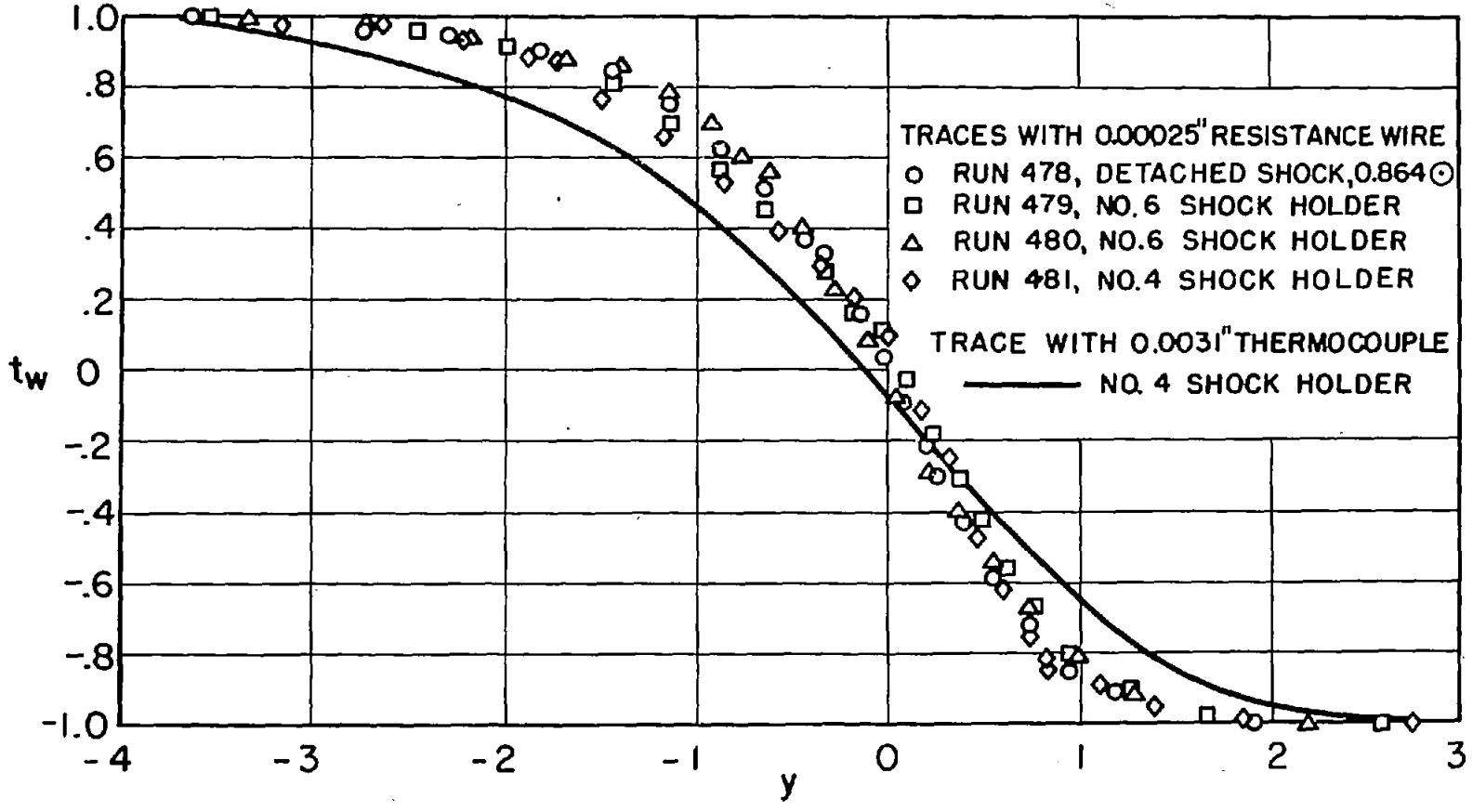

(g) Nozzle 8; 5.2 lb/hr; air; $M_1 = 3.70$.

Figure 9.- Continued.

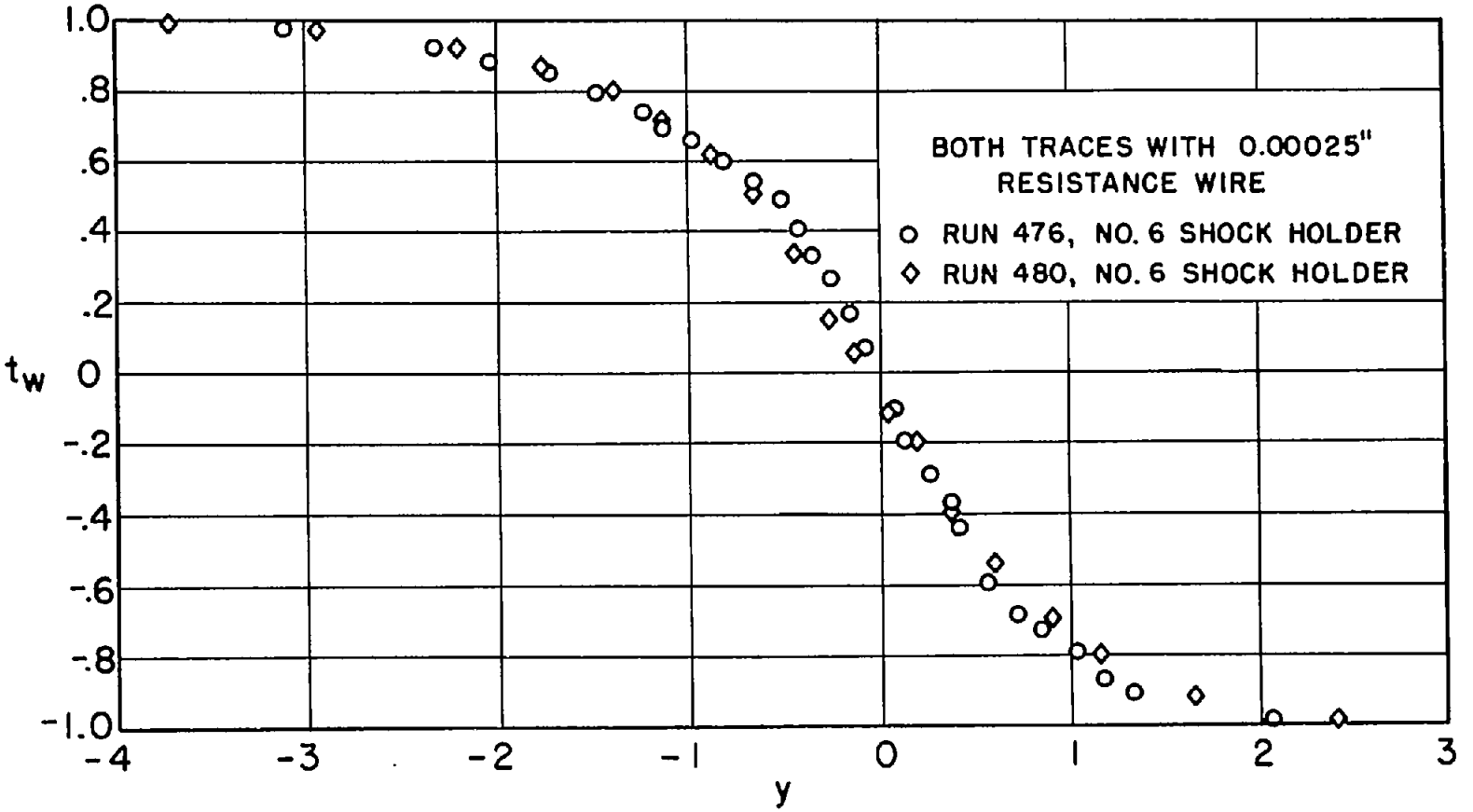

(h) Nozzle 8; 10.3 lb/hr; air; $M_1 = 3.91$.

Figure 9.- Concluded.

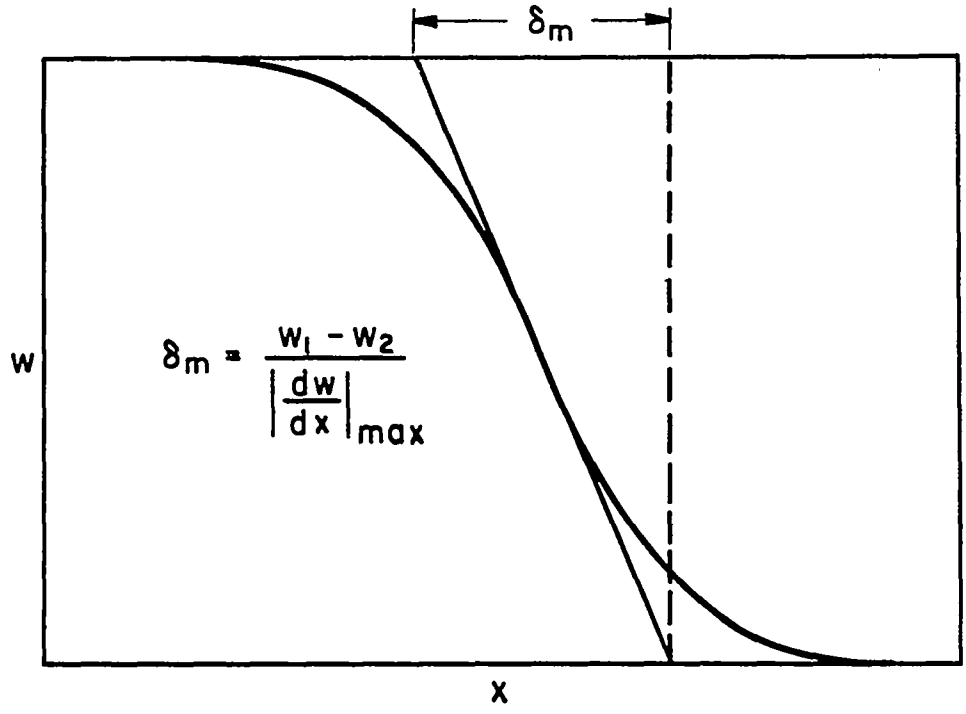

(a) Maximum-slope thickness.

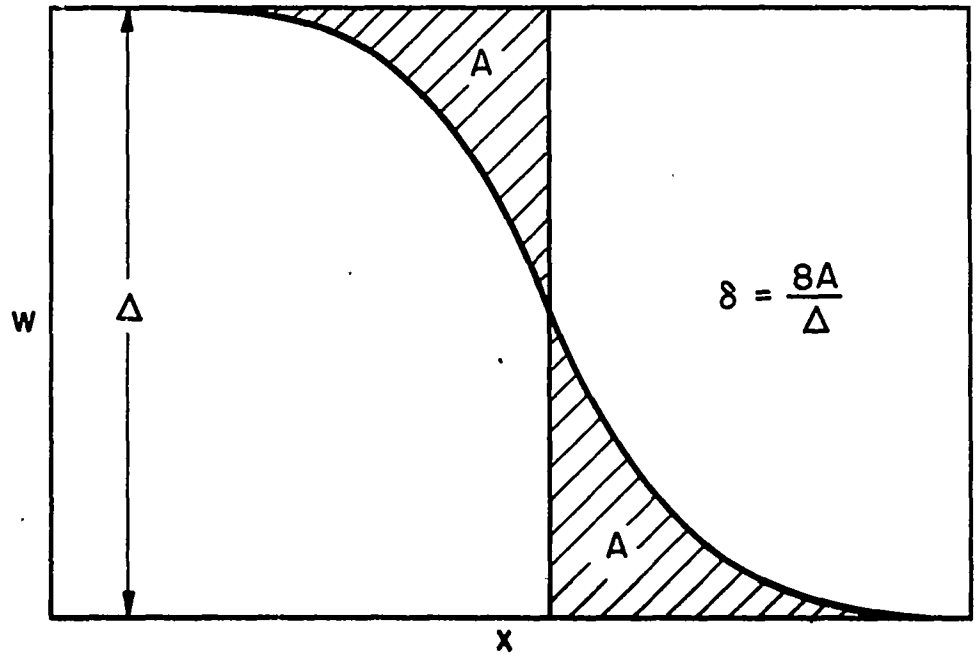

(b) Area thickness.

Figure 10.- Definitions of shock thickness.

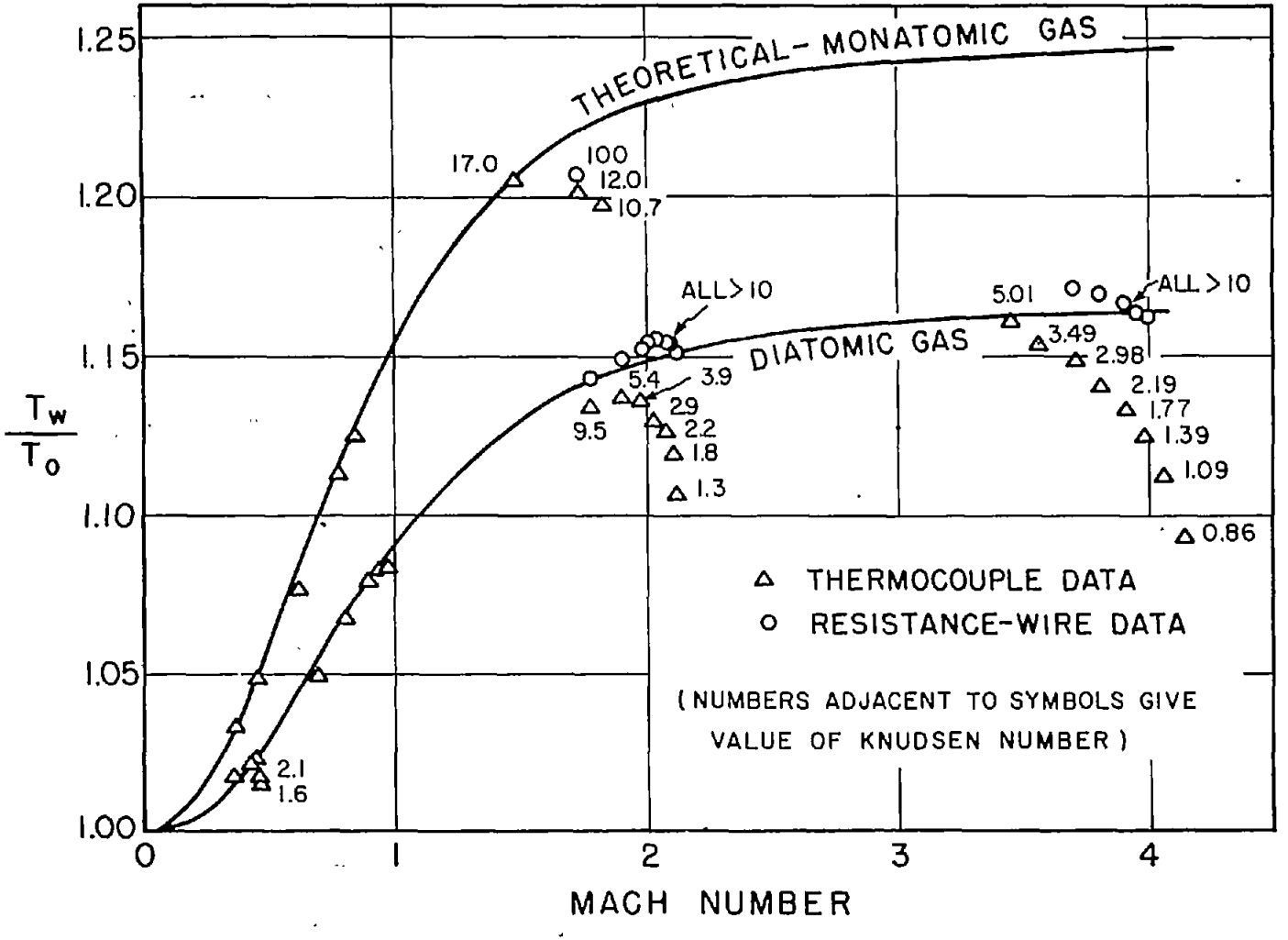

Figure 11.- Comparison of experiment and theory for cylinder temperature in uniform stream.

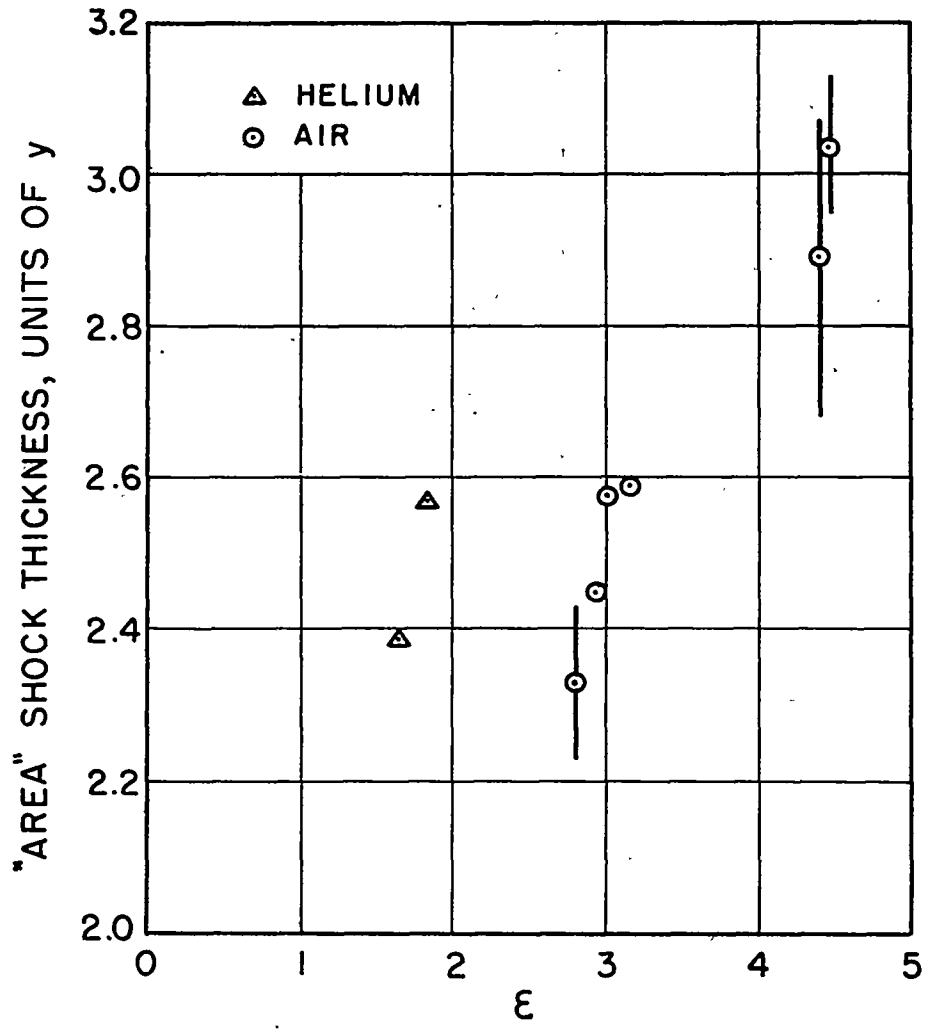

Figure 12.- Area shock thickness versus shock strength.

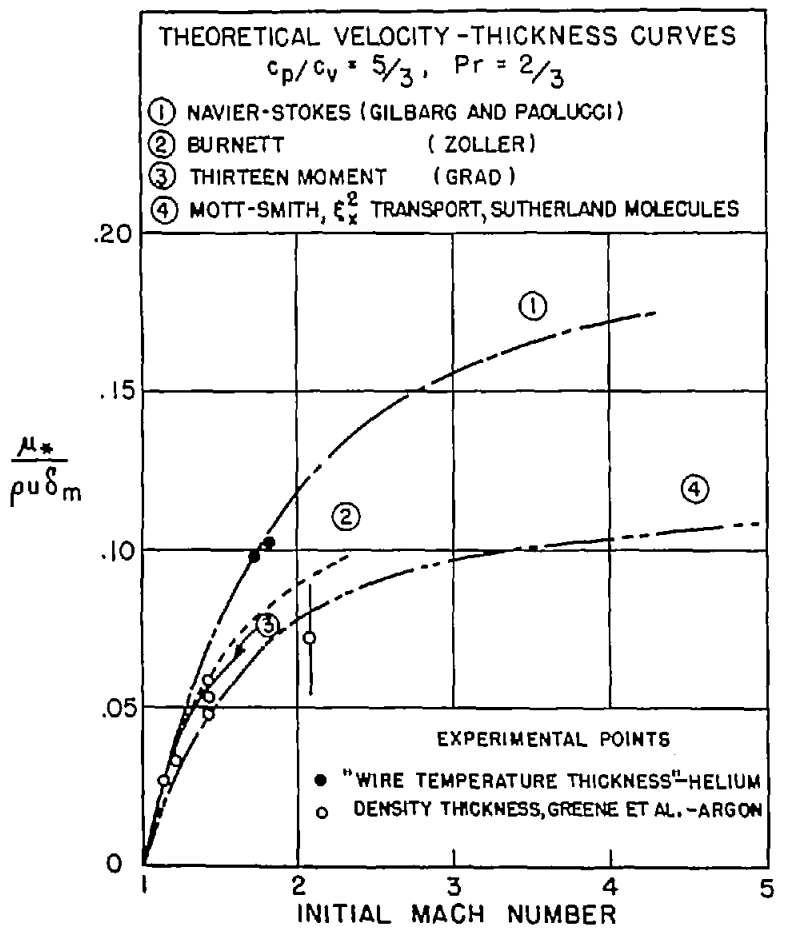

(a) Monatomic gas.

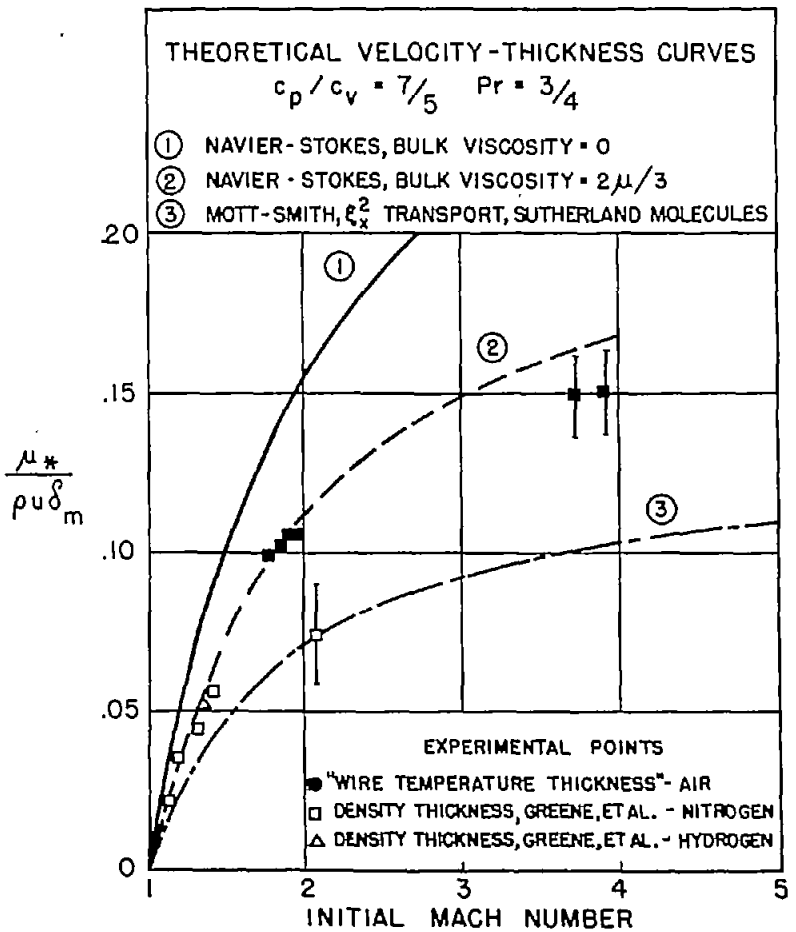

(b) Diatomic gas.

Figure 13.- Shock thicknesses.

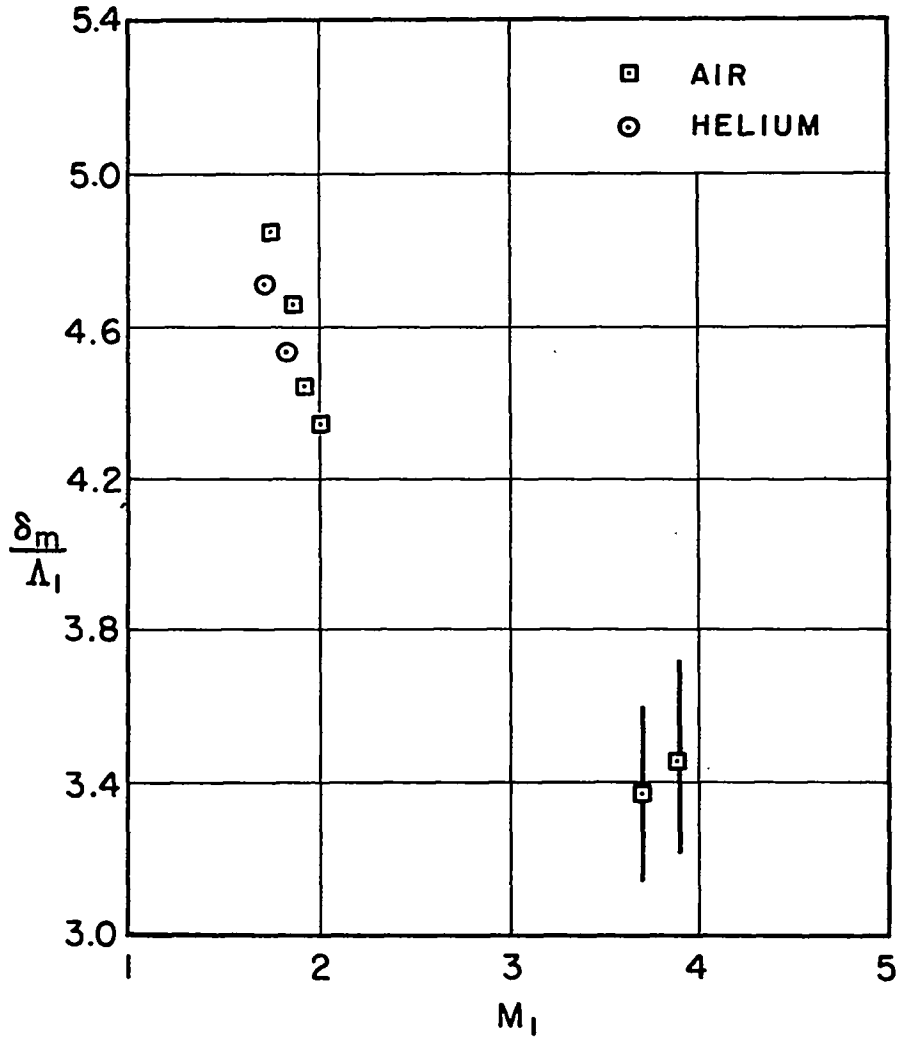

Figure 14.- Maximum-slope shock thickness in terms of upstream mean free path.

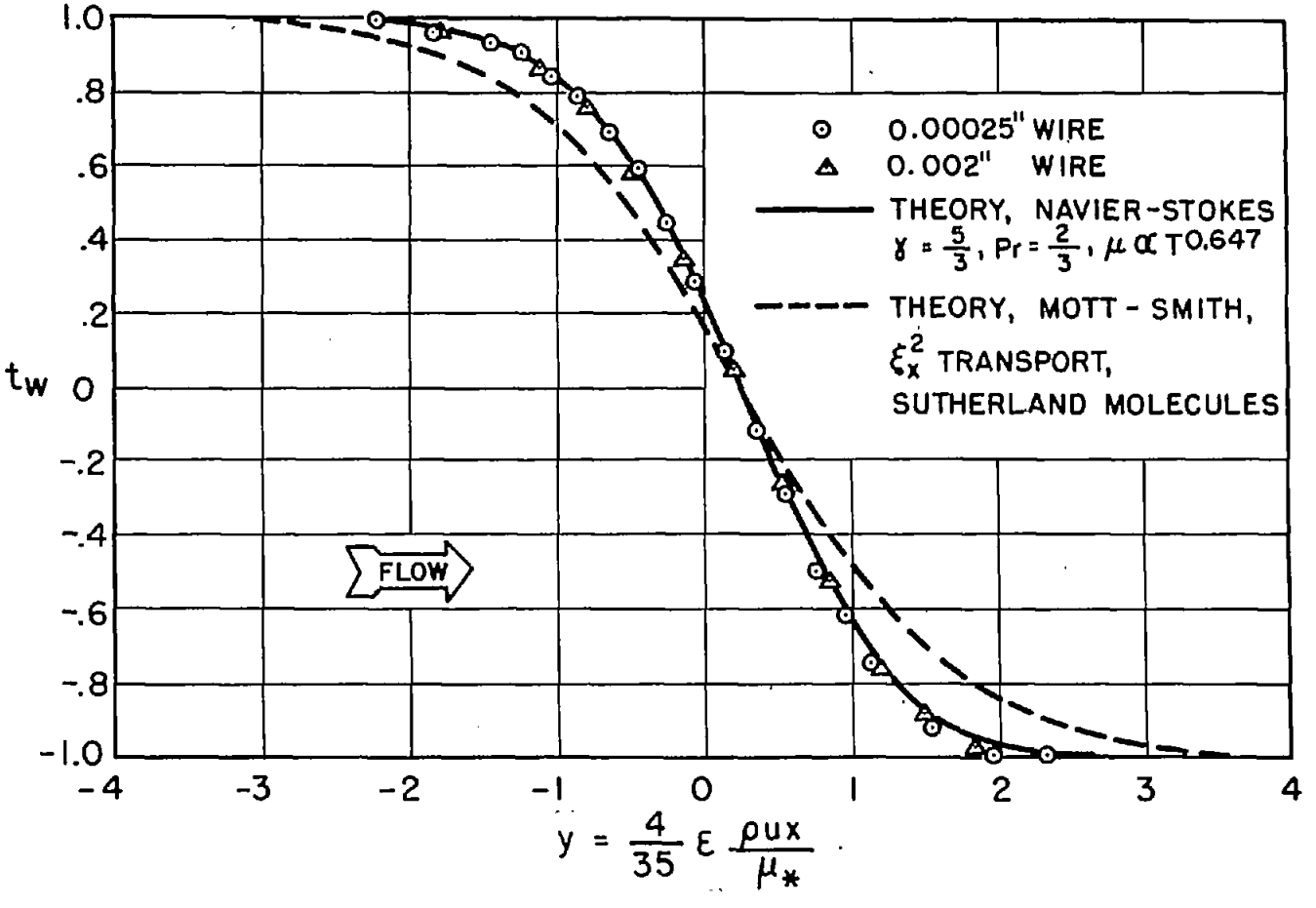

(a) Monatomic gas (helium); $M_1 = 1.82$.

Figure 15.- Comparison of experiment and theory.

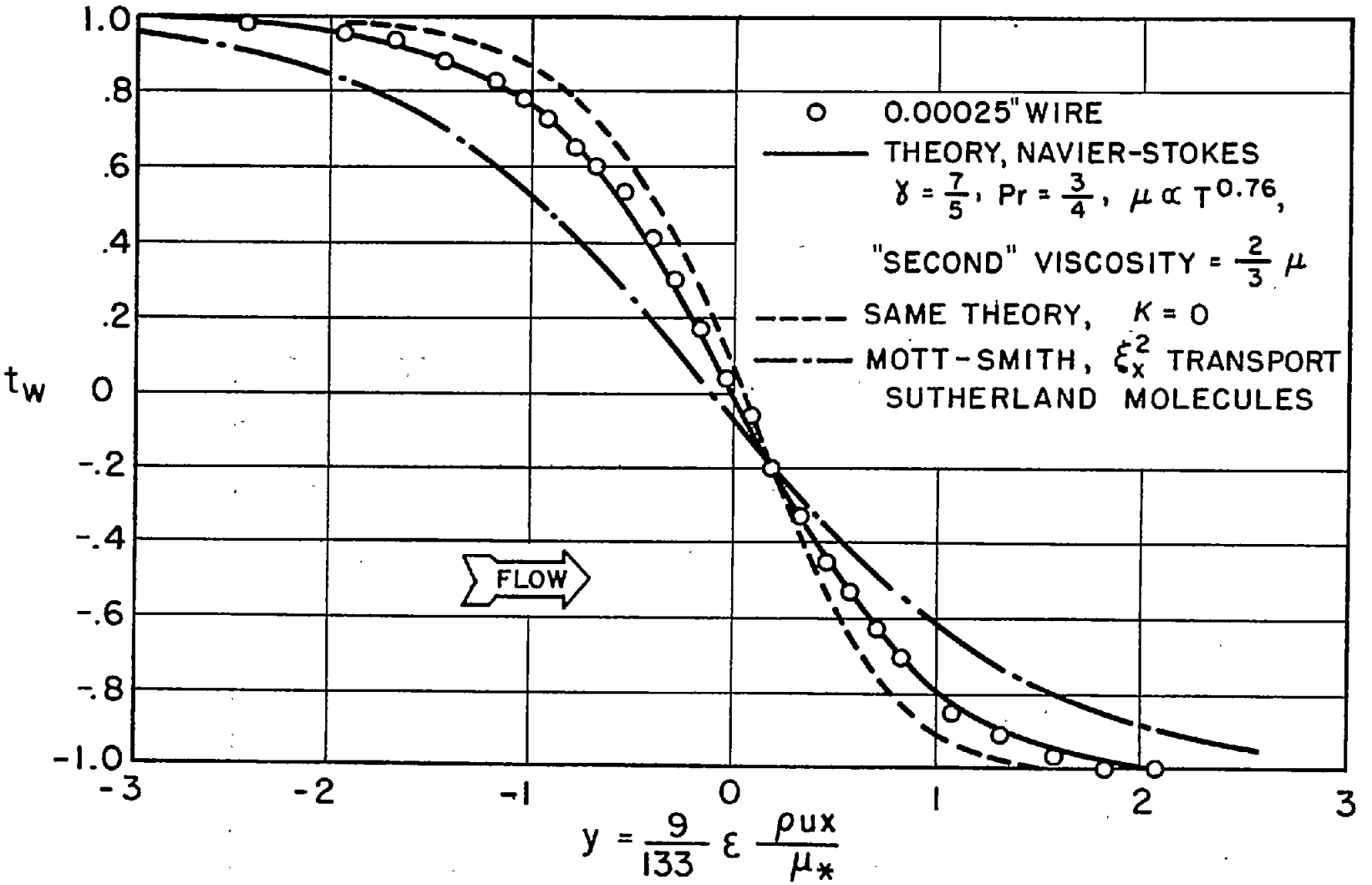

(b) Diatomic gas (air); $M_1 = 1.89$.

Figure 15.- Continued.

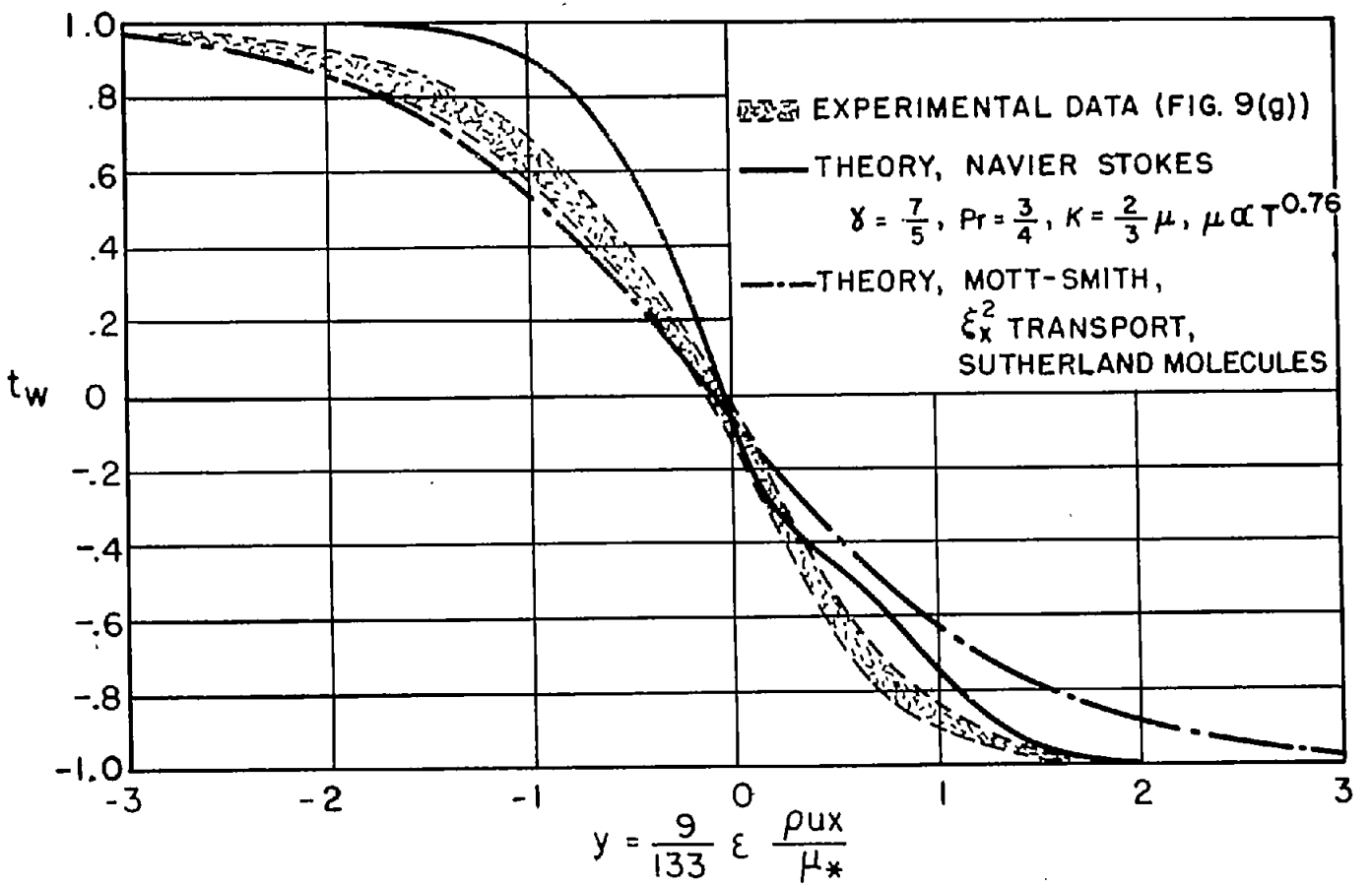

(c) Diatomic gas (air); $M_1 = 3.70$.

Figure 15.- Concluded.

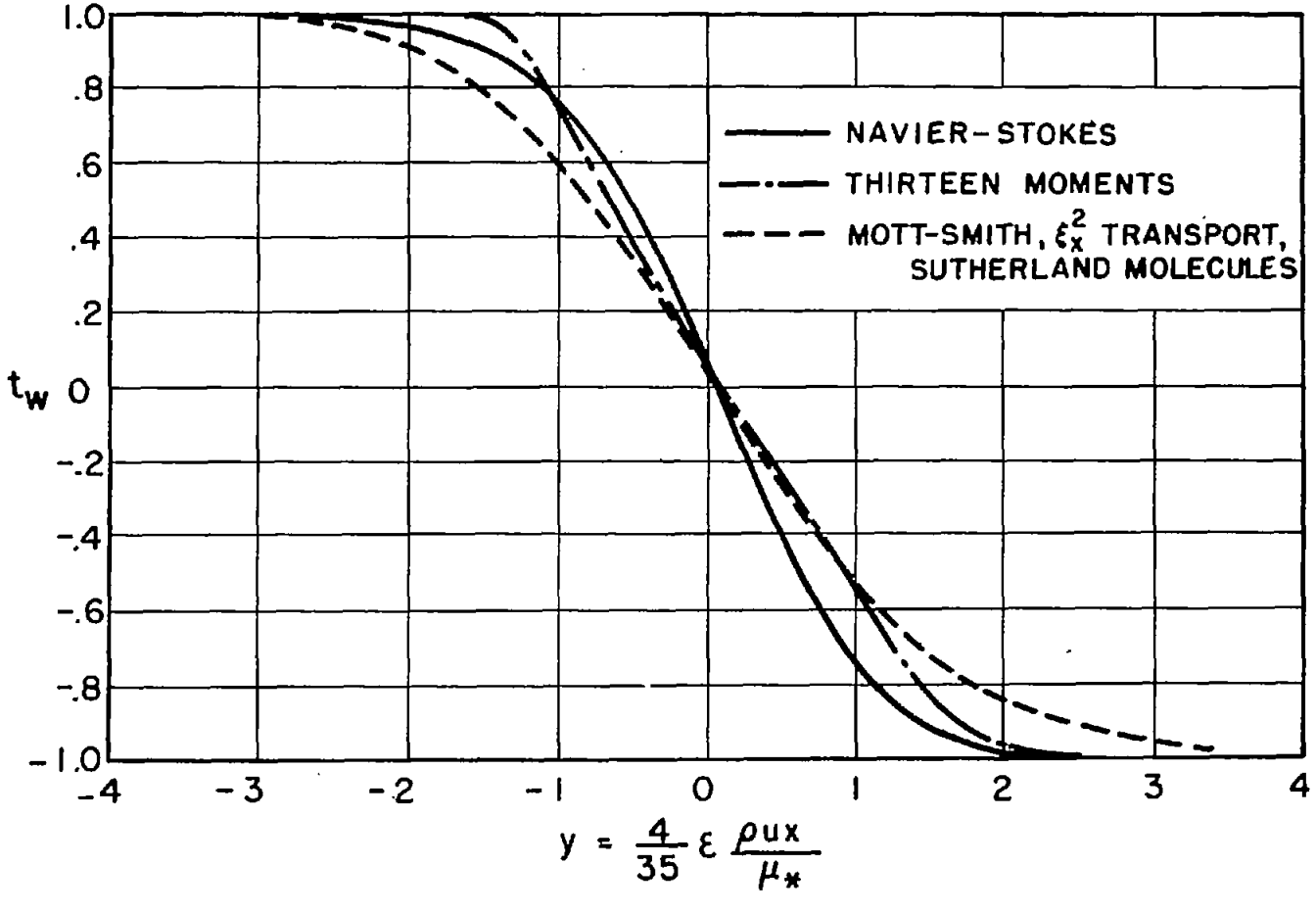

Figure 16.- Comparison of various theories for monatomic gas (helium). $M_1 = 1.61$.

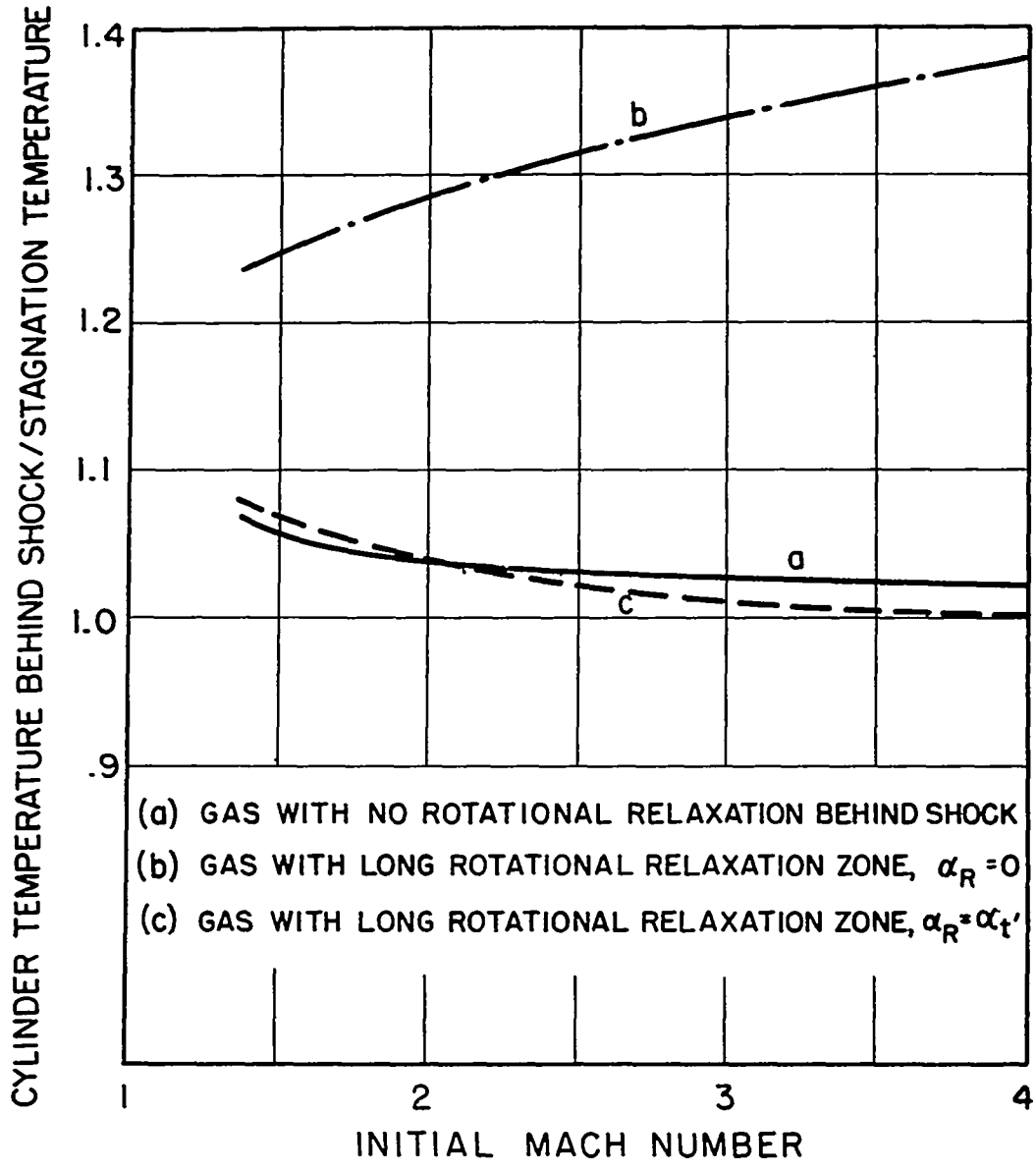

Figure 17.- Cylinder temperature behind a normal shock in a diatomic gas exhibiting rotational relaxation (appendix C).

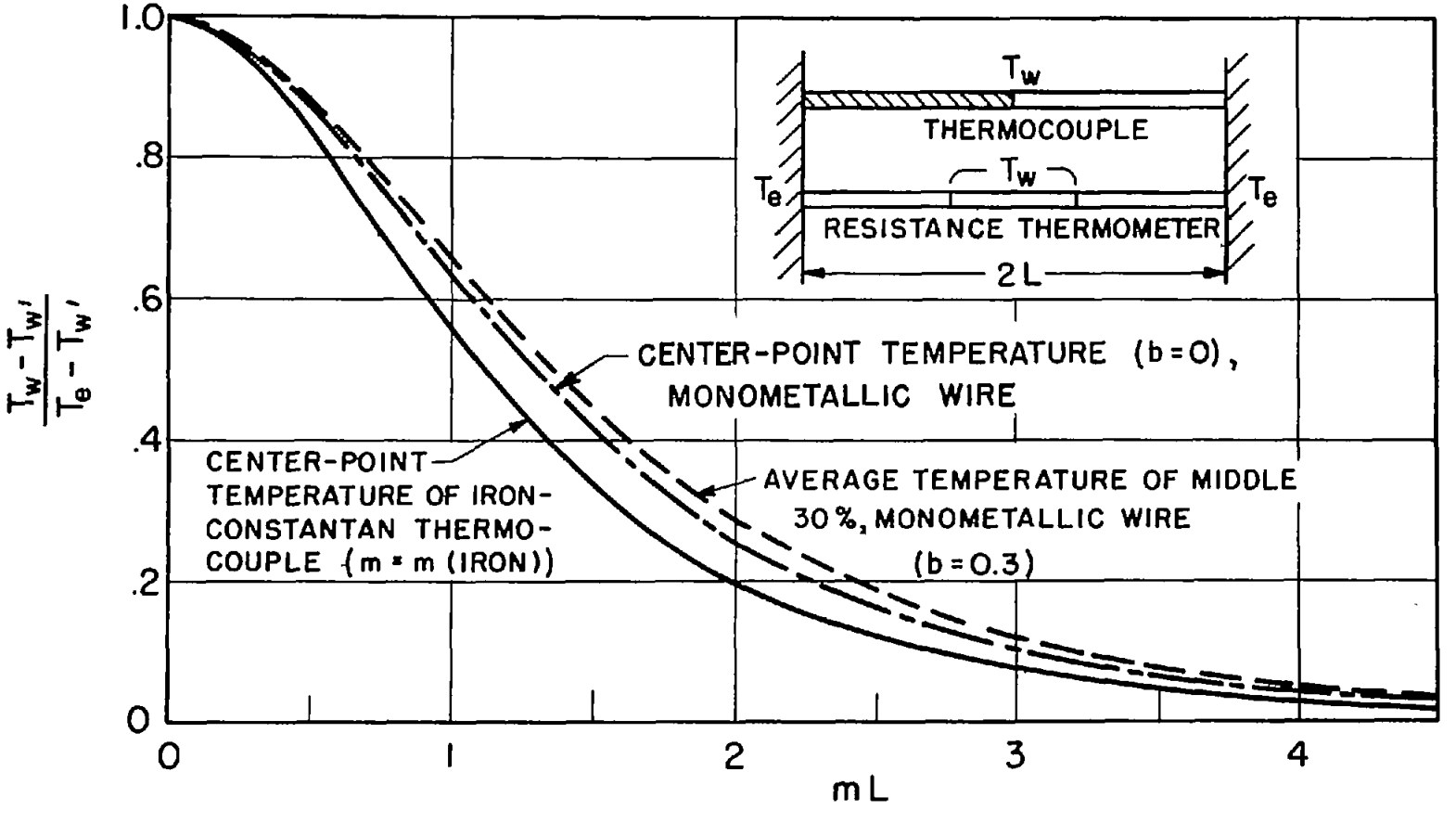

Figure 18.- Influence of end losses on thermocouple and resistance-wire probes.